LASER INTERFEROMETER GRAVITATIONAL WAVE OBSERVATORY

- LIGO –

CALIFORNIA INSTITUTE OF TECHNOLOGY
MASSACHUSETTS INSTITUTE OF TECHNOLOGY

Document Type **Technical Report**	**DCC Number** **LIGO-T010006-00-R**	January 25, 2001

Report to NSF on the TAMA-SAS Passive Seismic Attenuation Chain Test for the Tokyo University 3 meter Interferometer

M. Ando, A. Bertolini, G. Cella, R. DeSalvo, F. Fidecaro, M. Fukushima, S. Kawamura, G. Losurdo, S. Marka, K. Numata, V. Sannibale, F. Seve, K. Somya, R. Stanga, R. Takahashi, A. Takamori, H. Tariq, K. Tsubono, E. Ugas, N. Viboud, C. Wang, T. Yoda

Distribution of this draft: NSF reviewres, LIGO scientists
This is an internal working note
of the LIGO Project.

California Institute of Technology
LIGO Laboratory - MS 18-34
Pasadena CA 91125
Phone (626) 395-212
Fax (626) 304-9834
E-mail: info@ligo.caltech.edu

Massachusetts Institute of Technology
LIGO Laboratory - MS 16NW-145
Cambridge, MA 01239
Phone (617) 253-4824
Fax (617) 253-7014
E-mail: info@ligo.mit.edu

www: http://www.ligo.caltech.edu/

Introduction.

In fall 1999 the LIGO-SAS/Virgo-Superattenuators passive attenuation and inertial damping scheme was already a mature seismic isolation scheme and two technical implementation versions were ongoing.

The first, based on Magnetic Anti Spring filters, was ready for installation and operation in Virgo, it was being tested with inertial damping and controls, and it is going on line at this time.

The other, mechanically substantially more advanced, developed to suspend the Advanced LIGO optics and based on the LIGO Monolithic Geometric Anti Spring Filters (MGASFs) was undergoing mechanical tests in Pasadena.

The 2005 Advanced LIGO installation being far in time, a scaled, but interferometric test was deemed necessary to break-in the LIGO advanced passive attenuation technologies and provide a final validation test.

At the same time, the TAMA 300 interferometer operation had shown the inadequacy of its seismic attenuation system. The TAMA collaboration asked for assistance from the LIGO-SAS group in Caltech to design a suitable advanced seismic attenuation system and adopted the passive attenuation and chain modes inertial damping scheme.

In January 2000 it was agreed, between the LIGO SAS group in Caltech and the TAMA collaboration, to jointly design and build two SAS towers for a Fabry Perot test at the 3 meter facility at the University of Tokyo prior to the construction and installation of the four or five units for the TAMA 300 interferometer.

Design and construction of the new TAMA-SAS system was to be made in Caltech and a full-scale, full-system final acceptance test to be jointly performed in the Tokyo University 3 meter interferometer facility.

The TAMA SAS design was based on a small optics system already under study in Pasadena. It was decided to adapt a LIGO-SAS test tower to the TAMA requirements.

Summarizing, the tests in the 3 meter interferometer had a double raison d'etre.

For TAMA the 3 meter interferometer test was intended to validate the concept, debug the full-scale and complete attenuation towers in order to be able, later on, to rapidly install pre-assembled pre-optimized units keeping the TAMA interferometer offline for a minimum amount of time.

For LIGO the test was intended as a validation of the GASF SAS concept for Advanced LIGO (at the time LIGO II) and a subsequent cryogenic LIGO version of it.

The TAMA SAS is a scaled and less performing design of the LIGO SAS towers, fitting in the TAMA vacuum envelope and satisfying its requirements. The individual filter performance is higher than in the LIGO SAS initial prototype thanks to the adoption of the Monolithic GAS springs. The payload capacity was reduced by a factor of more than 30 to support the much lighter TAMA 1 kg mirrors. The size was reduced by a factor of two to fit in the existing vacuum envelopes. The downgrade in frequency performance was mainly caused by the reduction in pendulum length; the seismic attenuation that for LIGO was starting below 4-6 Hz for TAMA resulted at 10 Hz.

The TAMA 3 meter test was assigned as the Doctoral thesis object of Akiteru Takamori of University of Tokyo and was intended for implementation in the 3 meter vacuum system in the fall 2000.

Initially the TAMA-SAS tower was intended just as a seismic attenuation system supporting the existing TAMA mirror suspensions. In early summer 2000, it became clear that the existing TAMA mirror suspension box was inadequate for TAMA. Akiteru presented the problem to the TAMA collaboration and it was decided to start a crash development program merging the TAMA magnetic damping experience with the Virgo recoil mass concept and the LIGO MGAS technology into a double-pendulum, hierarchical-controls mirror suspension system. The Pasadena group has been assisting to speed up the mechanical realization of the new mirror suspension system.

This was a major expansion of scope of the 3 meter interferometer test and of the TAMA seismic attenuation and mirror suspension system (TAMA-SAS/SUS) but it made much better scientific sense. It also stretched the project time-scale by a few months.

To satisfy the additional mirror control requirements, the DSP based inertial damping and local control SAS system, developed for LIGO by Virginio Sannibale, was upgraded to a complete global control mirror interferometer control system.

The two TAMA SAS/SUS towers were built and are presently being assembled and tuned for cartridge installation in the 3 meter experiment.

The project also profited of the assistance of Virgo Superattenuator people and the support of the Pisa, Firenze, Urbino Universities.

System specifications

The specified performances of the TAMA SAS/SUS towers is summarized below:

- Payload 1 Kg, 10 cm diameter, 6 cm thick fused silica mirrors.
- Residual seismic attenuation above 10 Hz less than 10^{-18} m/Hz$^{1/2}$.
- Inertial damping of the rigid body motion of the chain.
- Residual r.m.s. motion of the mirror of less than 10^{-8} m (above 100 mHz).allowing an off-lock position stabilization to 10^{-8} m.
- In-lock longitudinal positioning from the interferometer’s length signal.
- Hierarchical mirror positioning controls.
- Passive magnetic damping of the rigid body motion of the multiple pendulum suspension.

- Fully digital local alignment control.
- Fully digital controls of the interferometer degrees of freedom (global controls).

TAMA SAS/SUS System Overview.

The TAMA SAS/SAS tower, see figure 1 and 2, consists of:

1. An Inverted Pendulum (IP) tuned below 30 mHz to:
   - Provide attenuation for the micro seismic peak
   - Provide a suitable base for the inertial damping of the chain body modes
   - Provide adequate sub-micron positioning of the attenuation chain suspension point.

The IP will be inertially damped and position controlled in its three degrees of freedom (the two horizontal translation and rotation around the vertical axis) by a diagonalized Multiple Input Multiple Output (MIMO) control system described later.

For these functions, the IP is provided with non contacting position sensors (LVDT), advanced electromagnetic linear force actuators and custom, low-frequency, high-sensitivity accelerometers.

The inertial damping, restricted in frequency below 5 Hz (well outside the frequency region of interesting sensitivity for TAMA 300), will also provide additional active attenuation of the micro-seismic peak noise.

2. A low frequency MGASF top filter operating below 200 mHz satisfying the same functions of the IP in the vertical direction. This top filter is provided with:
   - Vertical LVDT position sensor
   - Vertical actuation voice coil actuator.

   The LVDT/actuator of the top filter can be actuated in feedback mode to control the chain's vertical working point and dynamically reduce the filter's resonant frequency.
3. A fully passive vertical motion MGASF filter operating below 400 mHz to:
   - Provide passive attenuation in all six degrees of freedom
   - Support a recoil platform for the actuators pushing on the double pendulum control mass.

The double pendulum suspension point will be stable to less than 10^{-8} m r.m.s. above 100 mHz.

The double pendulum, figure 3 and 4, is composed of:

4. : A control mass supporting the double pendulum. It is provided with four mini MGAS springs, each supporting one of the suspension wires of the double pendulum intermediate mass. The control mass is driven by voice coil actuators whose magnets are on the control mass itself and whose coils are mounted on a cage rigidly connected to the filter above. The control mass also supports an auxiliary bob for the magnetic damping of the suspensions rigid body modes. The control mass can be actuated within a range much exceeding the expected mirror r.m.s. residual motion.

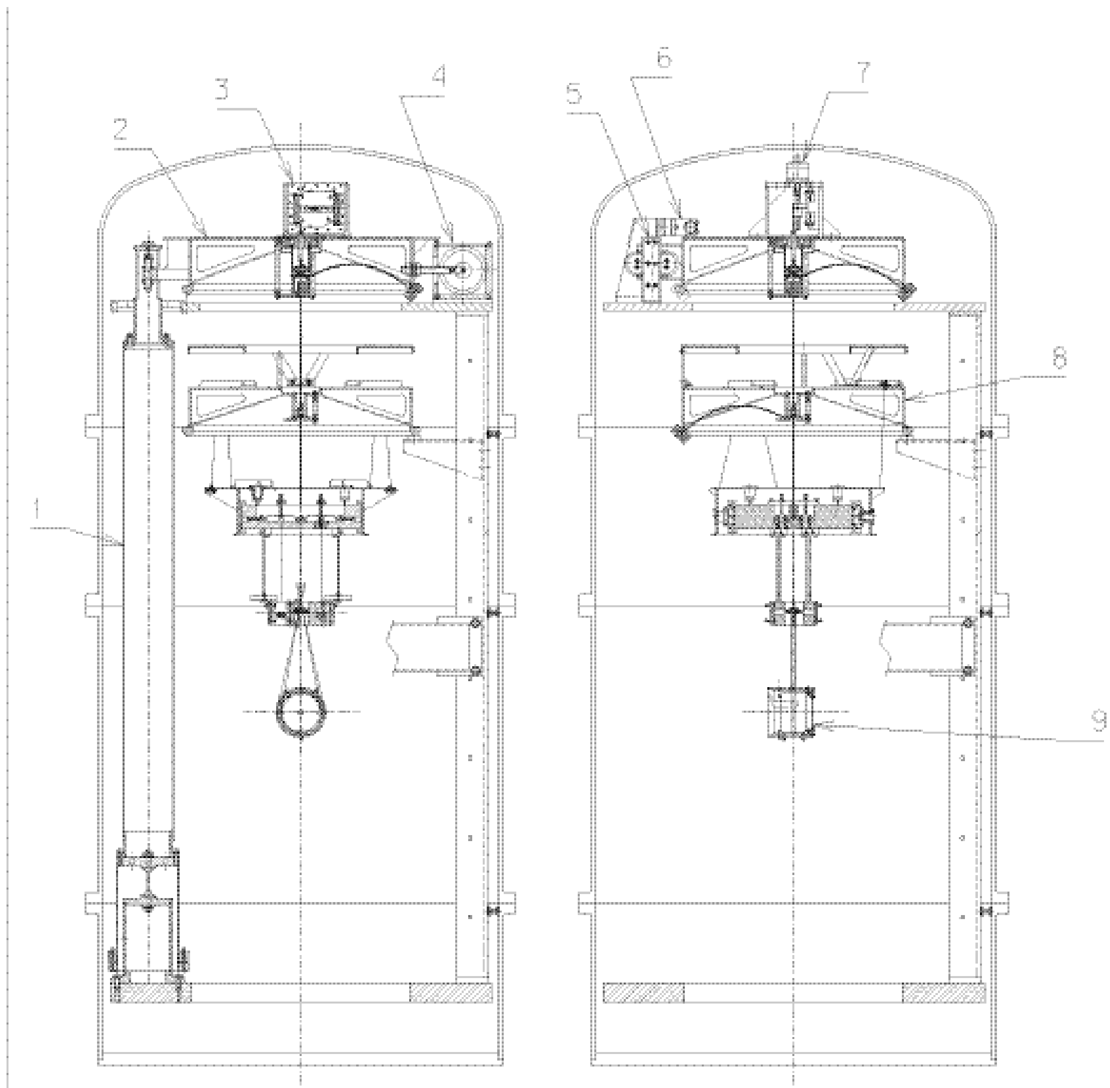

Figure 1: Front and side view of a TAMA SAS/SUS Tower. Visible: 1) inverted pendulum, 2) top MGAS filter, 3) accelerometer, 4) LVDT, 5) linear magnetic actuator, 6) horizontal motorized tuning spring, 7) vertical motorized tuning spring, 8) passive MGAS filter 9) mirror suspensions

Figure 2: Photos of the TAMA SAS tower prototype. Visible on top of filter zero are four accelerometers, the three at 120^{o} are the control ones, the fourth one is a diagnostic one.

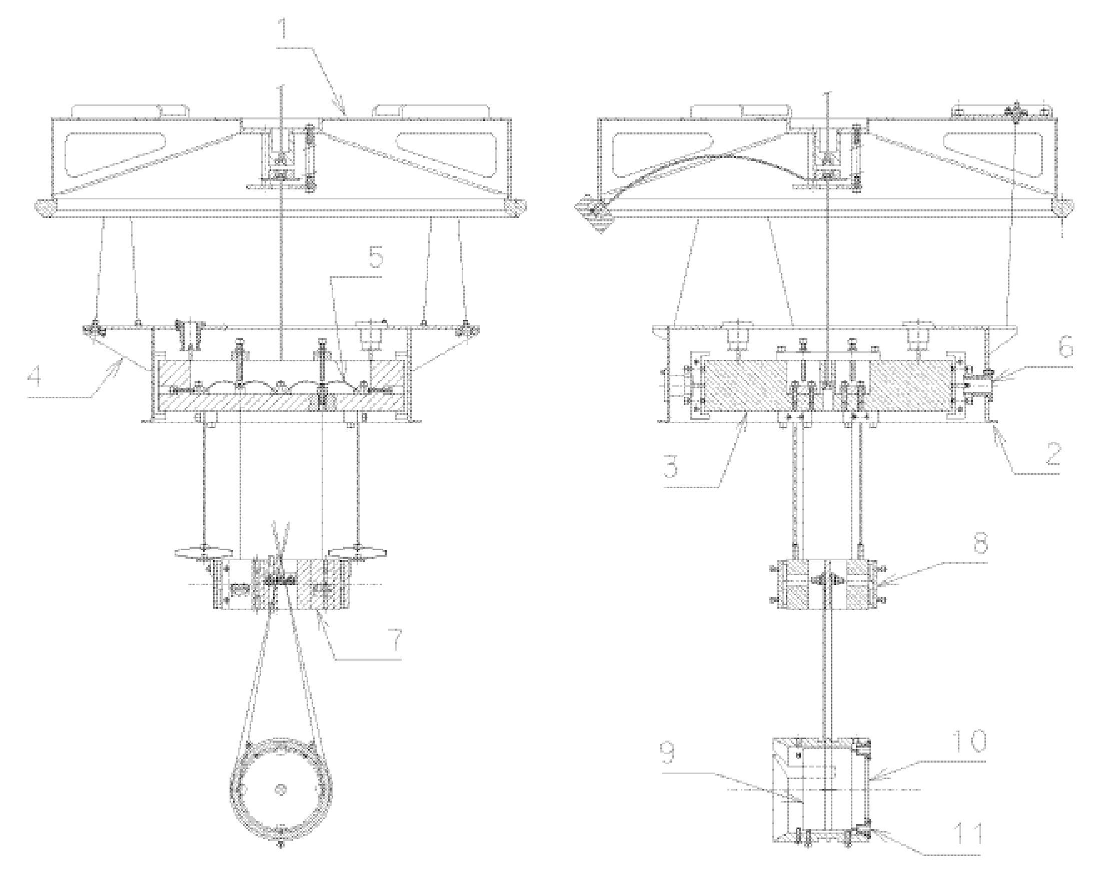

Figure 3: Double pendulum mirror suspension and control system hanging from a MGAS filter; front view on the left and side view on the right: 1) MGAS filter, 2) top mass control platform, 3) top mass, 4) control cage support structure, 5) mini MGAS springs, 6) control coils, 7) intermediate mass, 8) magnetic damping auxiliary bob, 9) mirror, 10) mirror recoil mass, 11) mirror control coils.

Figure 4: Exploded view of the new TAMA mirror suspension system.
In front a dummy mirror (aluminum cylinder at the center of photo), and its recoil mass (right) on their assembly stands with in between its red transportation cover. They will be both supported by an intermediate mass visible immediately behind the mirror on its left. The two central rectangular windows will house the mirror and recoil mass suspension wire clamps. The four small rectangular windows receive the four wires from which the intermediate mass is suspended from the top one. Behind the recoil mass, slightly on its left, is a rectangular box, which is the auxiliary bob and field shield for the magnets of the suspension passive damping. Between the magnet box and the mirror is the guitar tuning jig, used to precision suspending mirror and recoil mass from the intermediate mass. The double pendulum top mass is the large aluminum parallelepiped visible behind the mirror. Its two large slots house the twin tandem mini-MGAS springs (see figure 20). The top mass is surrounded by the control cage, visible on its left, which is rigidly connected to the preceding MGAS filter and pushes on the top mass by means of coils.
On the background is visible a Top Filter being tuned on its stand.

5. An intermediate mass which in its turn is supporting two four wire sets each suspending:
   - The mirror control recoil mass enveloping the mirror
   - The mirror itself
6. The one kg recoil mass is provided with four coils to control the mirror positioning and pointing.
7. The mirror itself in the 3 meter test is replaced by a dummy aluminum mass mimicking the TAMA 100 mm diameter mirror. The dummy mass contains a smaller mirror adequate for the 3 meter Fabry Perot test.

TAMA SAS/SUS Electronics

The electronics for the digital control, figure 5, is simply the Virgo electronics, designed by Diego Passuello and Alberto Gennai of INFN Pisa.
It is a VME based system comprising:

- floating point operations, 40 MHz, DSP card,
- 4 channel, 16 bit ADC card,
- 4 channel, 20 bit DAC card,

One set of DSP, ADC, DAC cards is used for each IP local control while an independent set will take care of the F.P. interferometer global control.

The electronics also includes the following NIM based, custom analogue modules:

- LVDT drivers
- Accelerometer drivers
- Coil drivers
- Stepper Motor Drivers

TAMA SAS/SUS Measured performances

Inverted pendulum:
The IP was independently tested. It was operated in air down to 12 mHz (figure 6). Tuning the IP to low resonances is reasonably easy. At 12 mHz even small changes of temperature and air currents substantially influence the residual spring constant, change the resonant frequency and change the IP working point. For this reason most tests were performed at or above 30 mHz where the IP resonant frequency is sufficiently stable even in air. In vacuum the IP performance will be much more reliable.

Figure 5: Photograph of the Virgo and TAMA digital control electronics. The three modules in the VME crate are the DSP, the ADC and the DAC cards generating the diagonalization matrices, the frequency filters and running an entire SAS tower local controls. A group of modules identical to these three will manage the interferometer global controls.

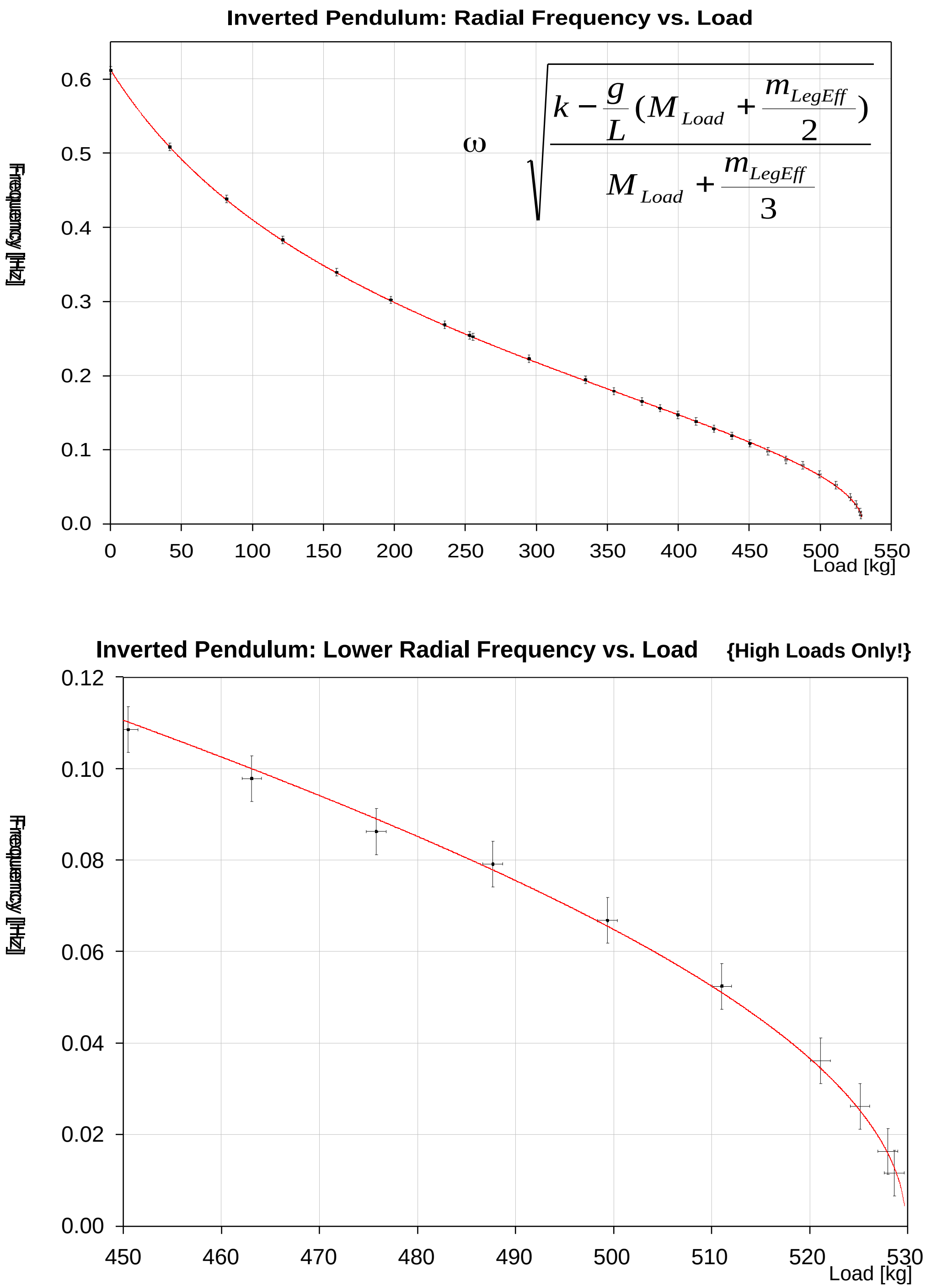

$$\omega = \sqrt{\frac{k - \frac{g}{L}\left(M_{Load} + \frac{m_{LegEff}}{2}\right)}{M_{Load} + \frac{m_{LegEff}}{3}}}$$

Figure 6: Tuning diagram of the LIGO Inverted Pendulum and expanded view of its low frequency end. Resonant frequencies of 10 to 20 mHz can be achieved also in the TAMA IP by tuning the IP load in 50 to 100 g steps.

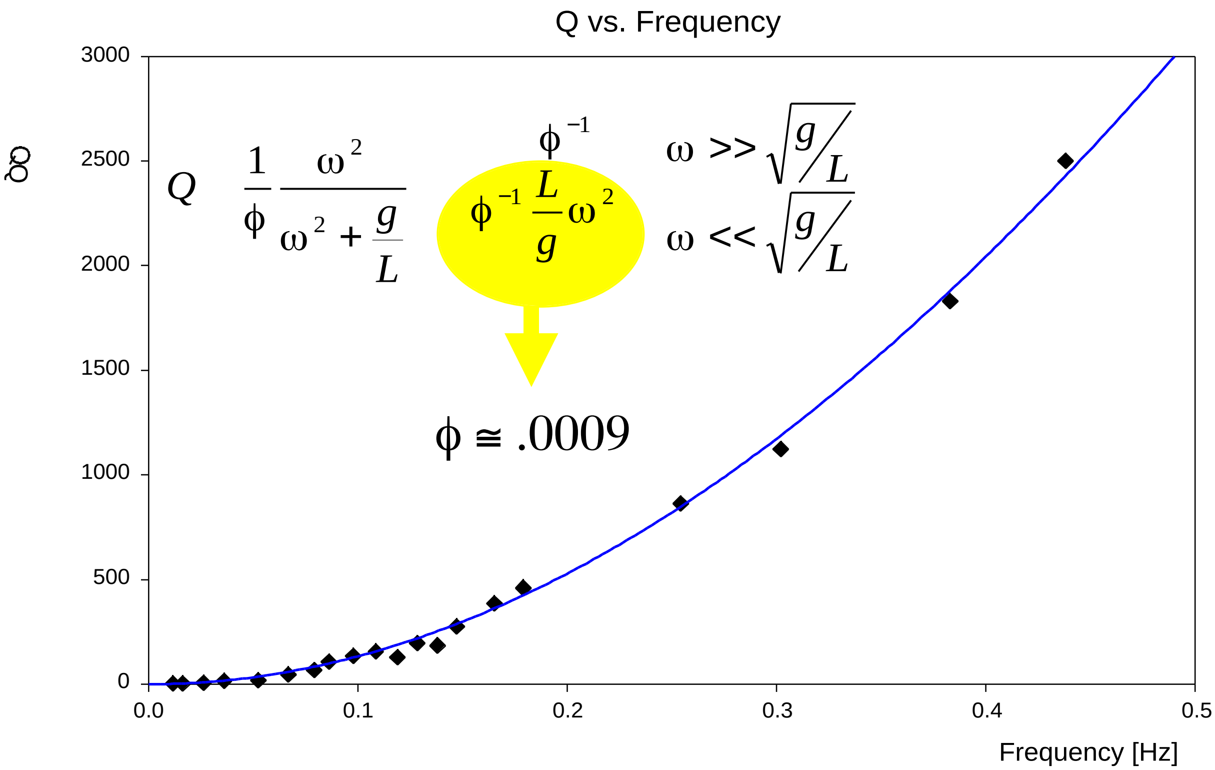

Figure 7: IP quality factor as a function of its resonant frequency. An IP tuned below 30 mHz presents a Q factor close to unity and hardly need damping.

It is interesting to note that at low frequency the IP resonance quality factor naturally drops to close to unity (figure 7). The inertial damping function may end up being restricted to the rotational mode, for the higher frequency chain modes, to provide tidal corrections and for additional off-band active attenuation of the micro seismic peak noise.
The tuning procedure for the IP counterweights was honed up to the level of achieving 80 dB passive attenuation at 10 Hz as shown in figure 8. The lowest IP frequency tunes are not achievable in the measurement setup because the oil bearing shaker used for calibration does not have the micro-radian pitch stability necessary at ultra low frequency.

MGASF top filter

The MGASF top filter was tuned to 200 mHz of vertical resonant frequency, it was tested for passive attenuation and measured a flat 60 dB attenuation up to more than 100 Hz as illustrated in figure 9, top. The attenuation figure shows no significant blade resonant peaks thanks to the cancellation effect due to the symmetry of the MGASF springs; as a comparison, figure 10 shows the comparatively inferior performance of a GASF and its blade resonances. Above 100 Hz, the filter body acts as the membrane of a loudspeaker and the measurement is dominated by acoustic coupling in the in-air measurements.
The top filter working point can be tuned by means of its motorized spring and by its voice coil. The filter's resonant frequency can be dynamically reduced by operating the voice coil in feedback with the LVDT.

MGASF standard filter

The MGASF standard filter is required to operate below 1 Hz of vertical resonance to match the pendulum frequency of the short suspension wires. It will be tuned to a very comfortable 300 mHz, in order to achieve the full filter's attenuation properties staring before 10 Hz. A MGAS filter tuning curve is shown in figure 11. At 300 mHz the filter tuning is straightforward and the vertical working point thermal drift is not a relevant issue (300 μm/ºC) and could be compensated with a bimetal blade if necessary. The filter was measured to achieve flat 55 dB attenuation up to above 100 Hz also without significant blade resonant peaks (figure 9 bottom).

Multiple pendulum top mass, mini MGAS suspension.

The double pendulum top mass attitude is controlled by means of coils, mounted on a control platform rigidly connected to the filter above, acting on permanent magnets.
The top mass houses four mini MGAS springs supporting the mirror and its recoil mass through an intermediate mass. The mini-MGAS springs can be tuned below the Hertz.

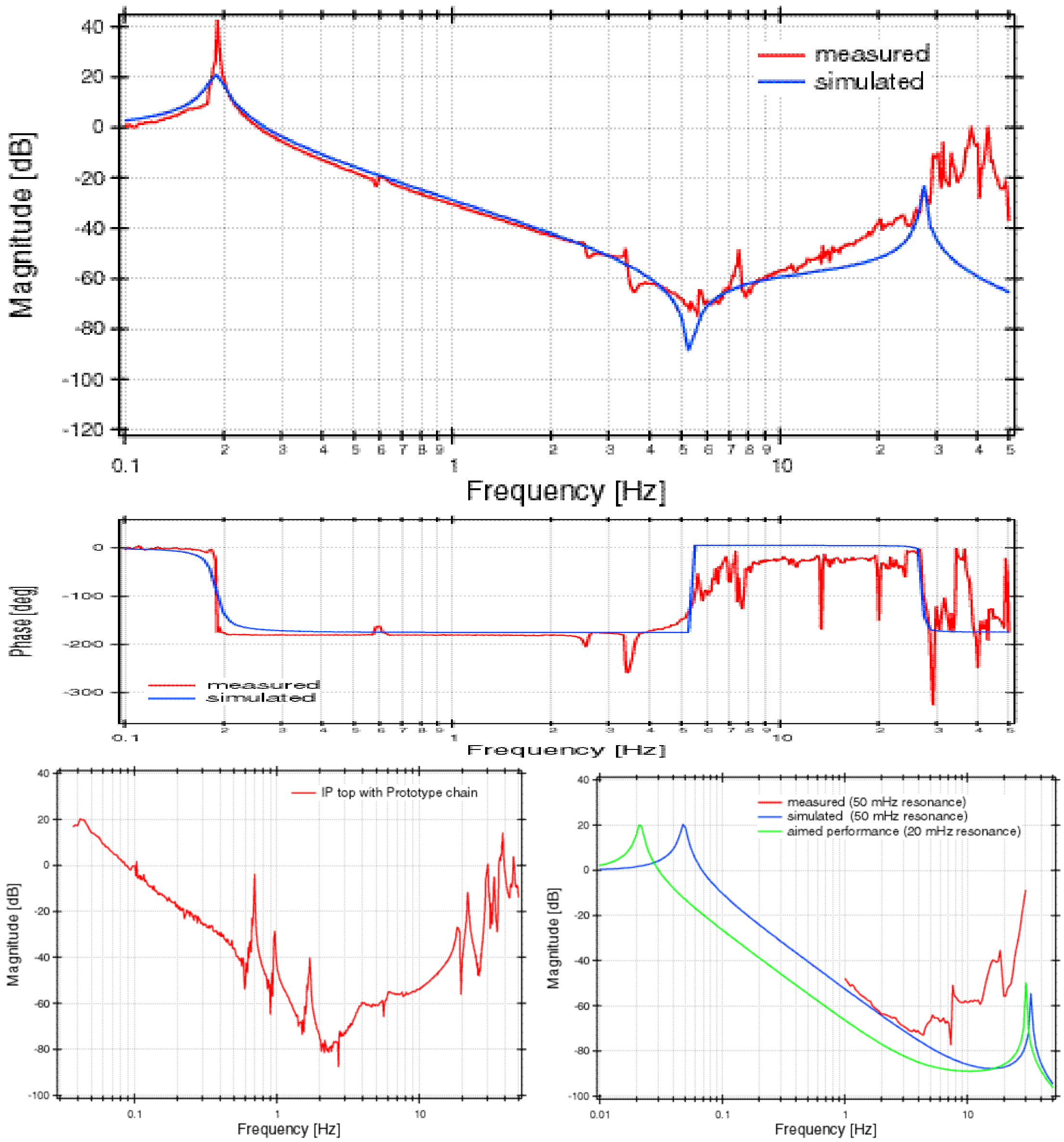

Figure 8: Passive attenuation performance of the TAMA IP. The two top figures are the transfer function and the phase of an IP with non-optimized counterweight. For measurement convenience reasons the IP resonant frequency was tuned at 200 mHz. The plateau above the 0.5 Hz notch is masked, in part, by noise in the brick stack loading the IP filter. The structure at 20 Hz is the resonance of the small joints connecting the IP leg to the F0. A nearly correctly counterweight and a lower IP frequency tune generate up to 80 dB attenuation at 1 Hz and more than 40 dB at the micro-seismic peak as illustrated in the bottom two graphs. The left bottom graph shows the effect of replacing some of the bricks with the SAS attenuation chain that produces the peak and notches structures between 0.5 and 2 Hz. These peaks are the ones that will be damped by the active damping system.

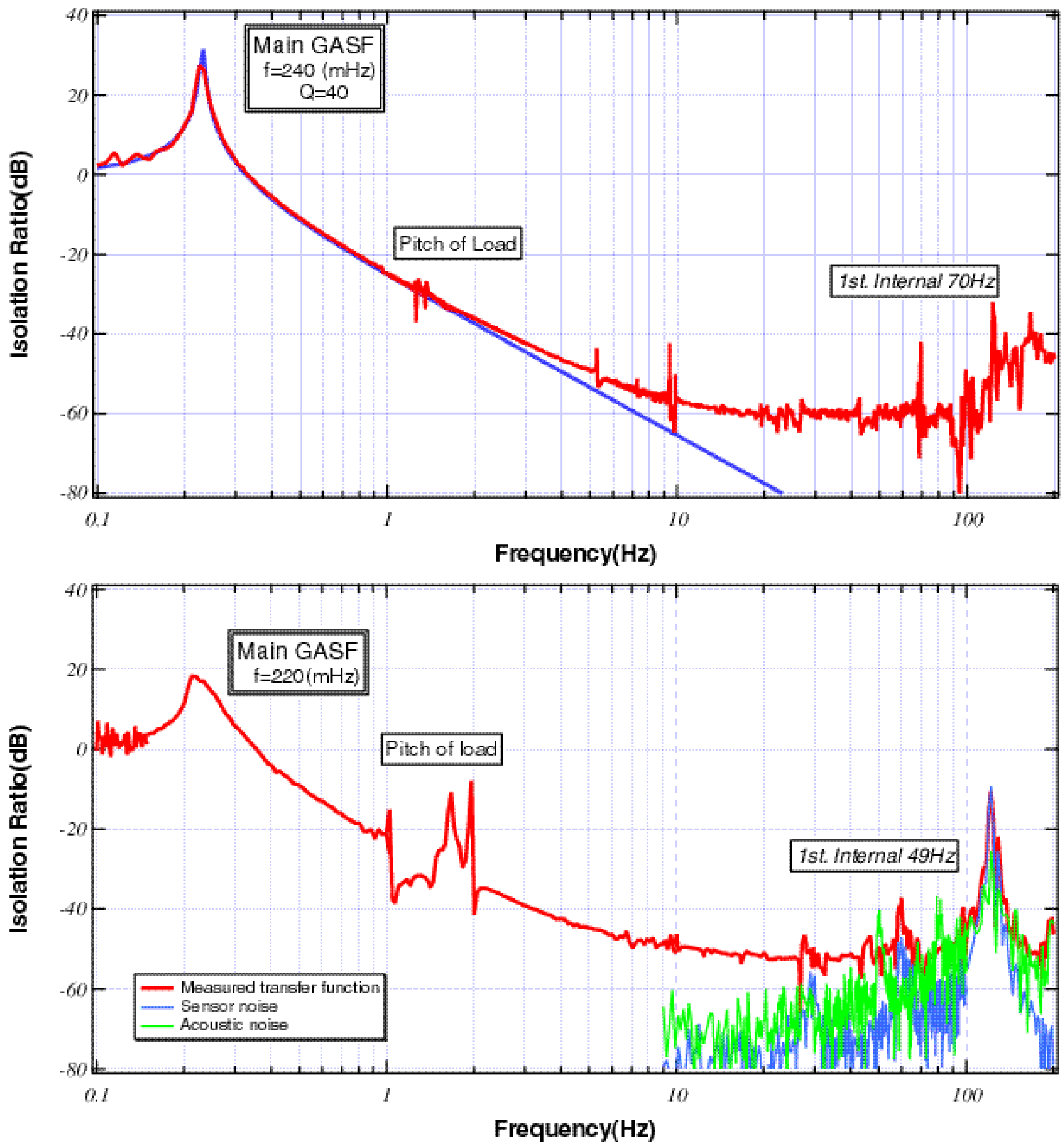

Figure 9: Attenuation properties of a MGAS filter with 2 mm thick blade (IP filter, top graph) and 1.5 mm thick (normal filter, bottom graph). The attenuation behaves like $1/f^2$ from the main GASF resonance to a plateau of 60 dB for the 2 mm thick blade and 55 dB for the thinner blade. The apparent width of the GASF resonance at 0.2 Hz depends on the measurement. The structures about 1 Hz are simply payload pitch modes. No blade resonances are visible (the corresponding resonances are at 70 or 49 Hz respectively, please confront with the peaks at 52 and 89 Hz in earlier versions of non monolithic GASFs in figure 10). Both measurements are dominated by acoustic couplings on the filter body and noise induced in the sensors above 100 Hz (green and blue lines).

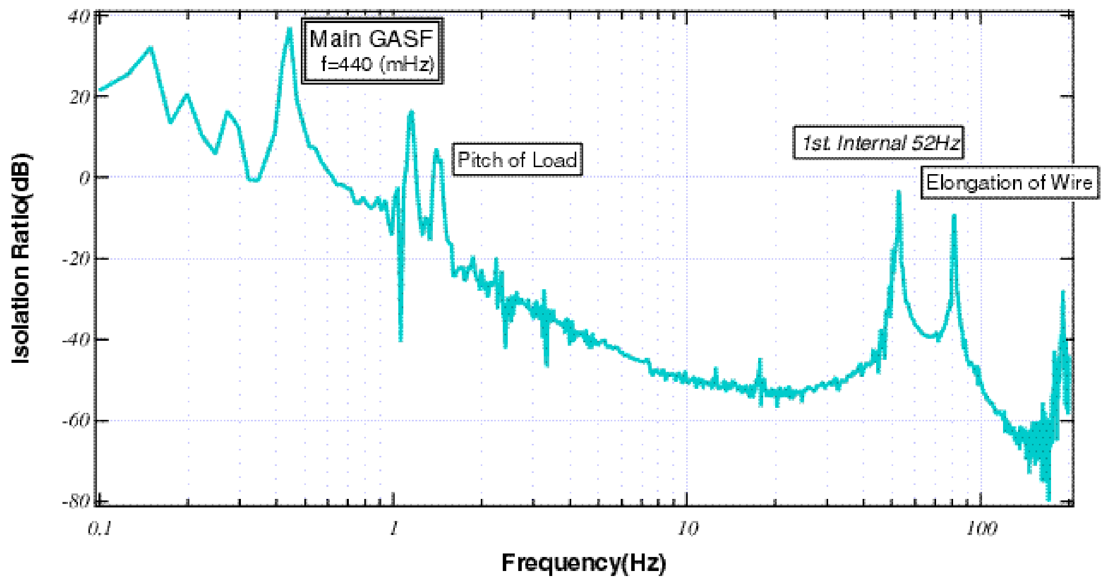

Figure 10: Attenuation properties of an earlier version, non monolithic GAS filter. Note the blade resonances at 52 and 90 Hz. They are present because the individual GAS blades are independently attached to a payload disk via a connection wire. The blade's internal resonances transmit seismic noise and necessitate resonance dampers as implemented in Virgo. In the monolithic GAS the blades are all connected together and their resonances have a node at the payload suspension point. The bad resonance effects are neutralized in MGASFs.

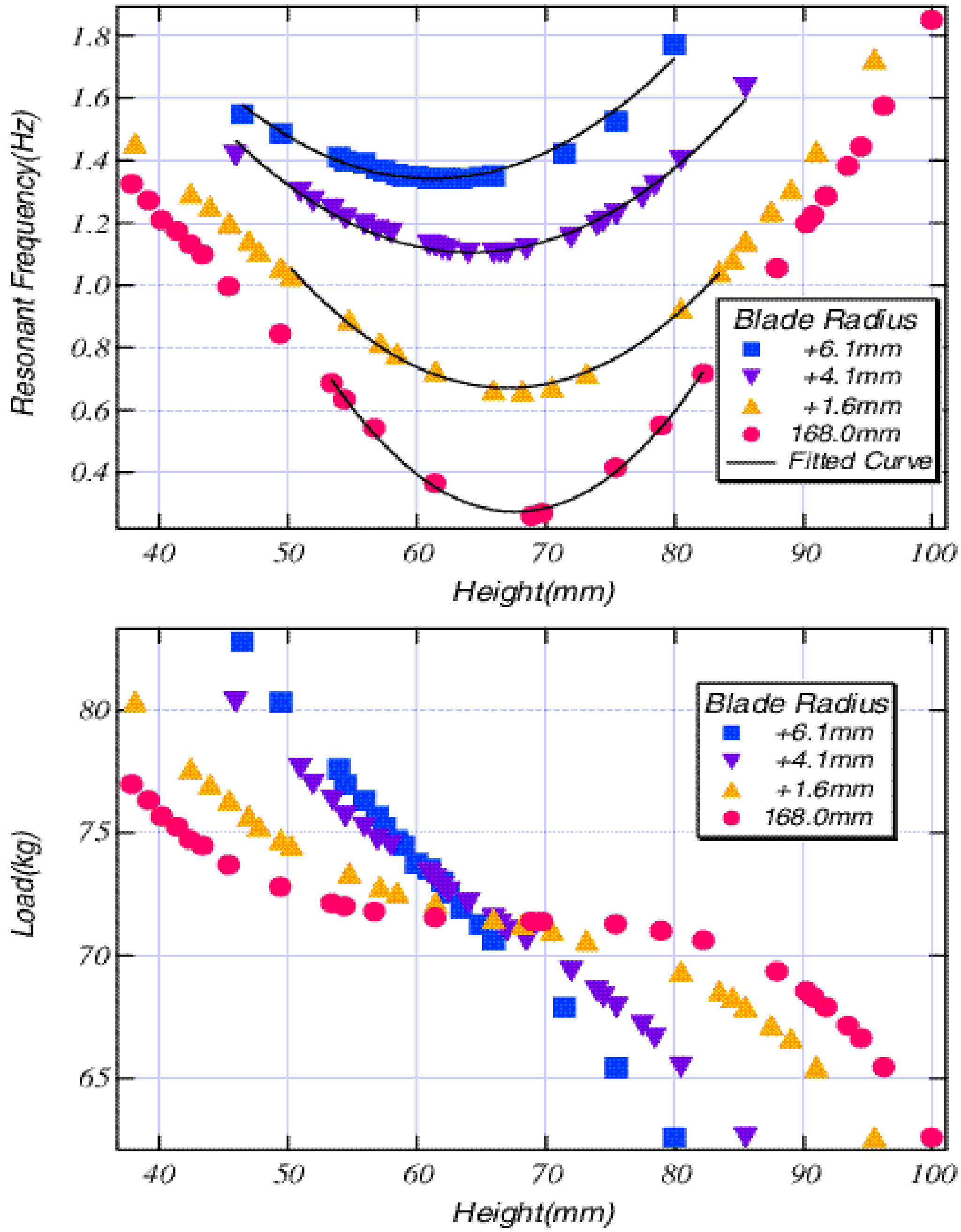

Figure 11: Frequency tuning curve for a MGAS filter. The Frequency versus vertical working point behavior and the working point versus is load are shown for different filter tunings. The vertical resonance at the working point (height 67 +/- 5 mm) is tuned by radially compressing the MGASF blades by different amounts. Vertical resonant frequencies below 1 Hz match the pendulum resonant frequency of the 30 cm long wires between the filters. The MGASFs present very good thermal stability.

LVDT position resolution

The chain suspension point is required to be positioned in space with a precision of less than 0.1 micron in order not to exceed the requirements imposed by mirror actuator dynamic range. Simulations show that TAMA SAS should achieve a payload r.m.s. even ten times better. To achieve this goal the LVDT position sensor, shown in figure 12, must have a matched resolution. (Of course during lock mode the LVDT signal is disregarded in the longitudinal direction in favor of the interferometer length error signal). The LVDT must present good linearity and resolution. The linearity has been achieved by mounting two receiver coils in Maxwell pair configuration (a configuration similar to an Helmoltz pair one, but where the field gradient uniformity is optimized, rather than the field amplitude, suggested by Lee Holloway). A signal linearity better than 1 percent over 25 mm dynamic range was achieved as shown in figure 13. A resolution of 20 nm/$Hz^{-1/2}$ was achieved as shown in figure 14. A further improvement in the electronics noise has subsequently improved the LVDT resolution by a factor of five.

Advanced Linear Magnetic Drive linearity

The inertial damping and the dynamic positioning of the payload requires the use of a non-contacting actuator. In order not to re-injecting noise in the chain, the actuator must generate a force independent of its own working point in the horizontal plane. Additionally, if the generated force was to change significantly for different IP positioning, the drive matrix would be position dependent.

The actuator developed for this use is a modified voice coil. The actuator force uniformity along the force direction is obtained using a suitably shaped magnet yoke. The actuator force uniformity perpendicularly to the force direction is achieved by using a flat coil much longer than the yoke width. Uniformity much better than a percent was achieved both along the force direction, as shown in figure 15, and across it over more than a square centimeter.

Accelerometers sensitivity

In order to provide inertial damping of the attenuation chain’s resonances (all between 03 and 3 Hz) it is necessary to have low frequency accelerometers of sufficient sensitivity. Getting enough sensitivity, and even to exceed requirements, is comparatively simple to do. If an accelerometer is sensitive to accelerations on any of the other 5 degrees of freedom, the acceleration signal in the “wrong” directions would be injected in the control loop and would be difficult to “diagonalize” it out. This may generate feedback stability problems. For this reason it is necessary to develop accelerometers which are sufficiently insensitive to the five orthogonal d.o.f..

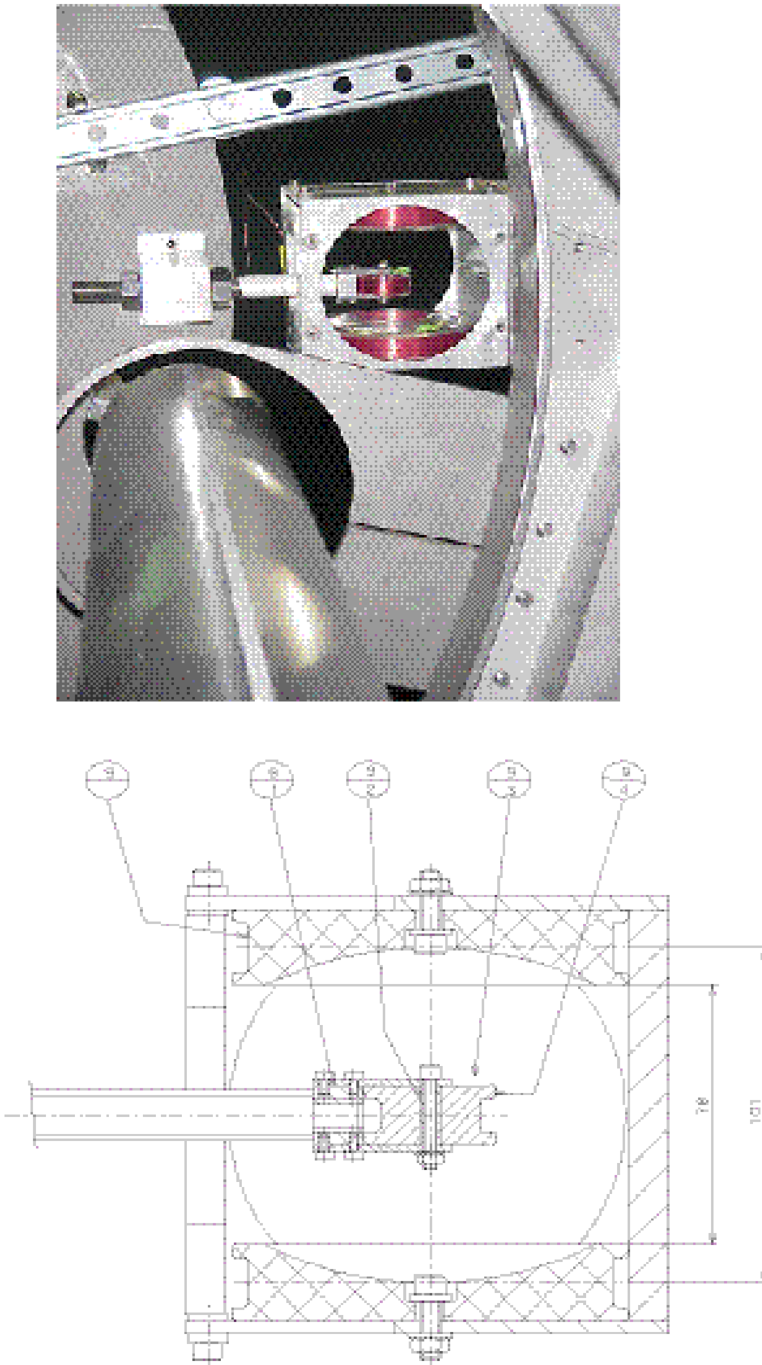

Figure 12: Photo and schematics of an LVDT. The small coil at the center is excited at 10 to 20 kHz signal and the twin large coils, wound in opposite directions and connected in serie, act as receivers and produce an electric signal proportional to the emitter's displacement from the geometrical center. This LVDT and its driver are exact replicas of the Virgo ones.

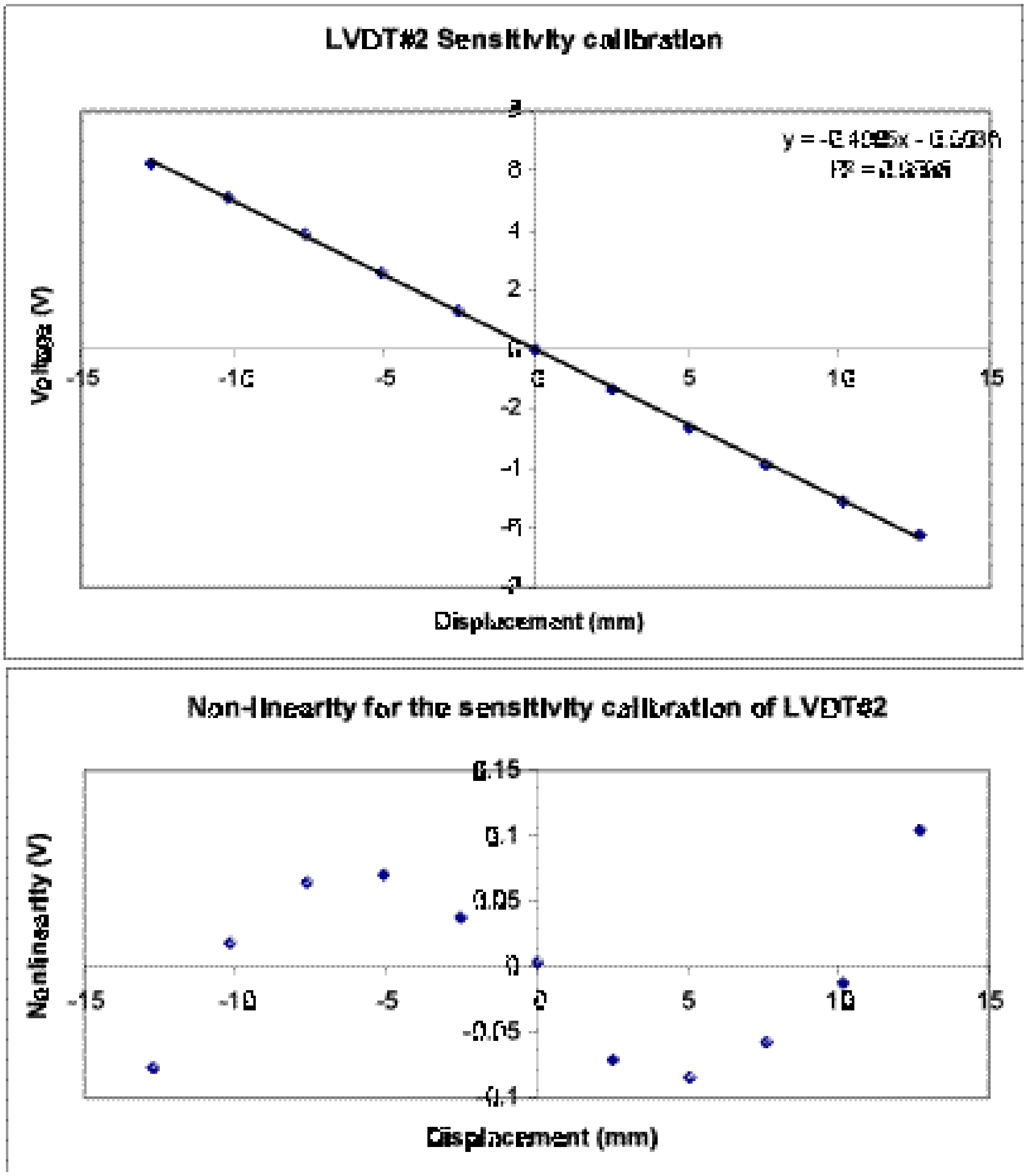

Figure 13: LVDT position response. Thanks to the Maxwell pair configuration of the receiver coils, the LVDT is linear within 1% over a range of 25 mm.
The Maxwell pair configuration is also very insensitive to transversal displacements.

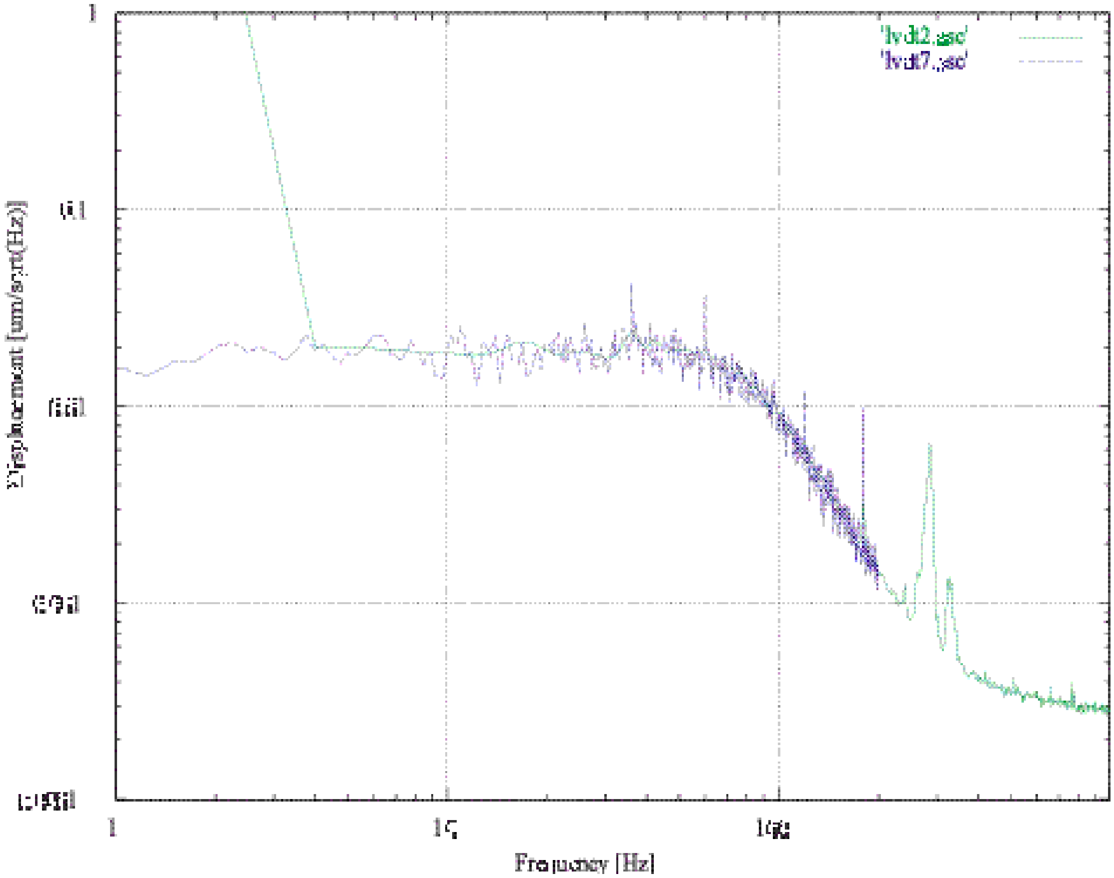

Figure 14: LVDT position resolution. A resolution of 20 nm/Hz$^{-1/2}$ is shown in figure. Subsequent electronics improvements have improved the sensitivity by a factor of 5, to below 5 nm/Hz$^{-1/2}$.

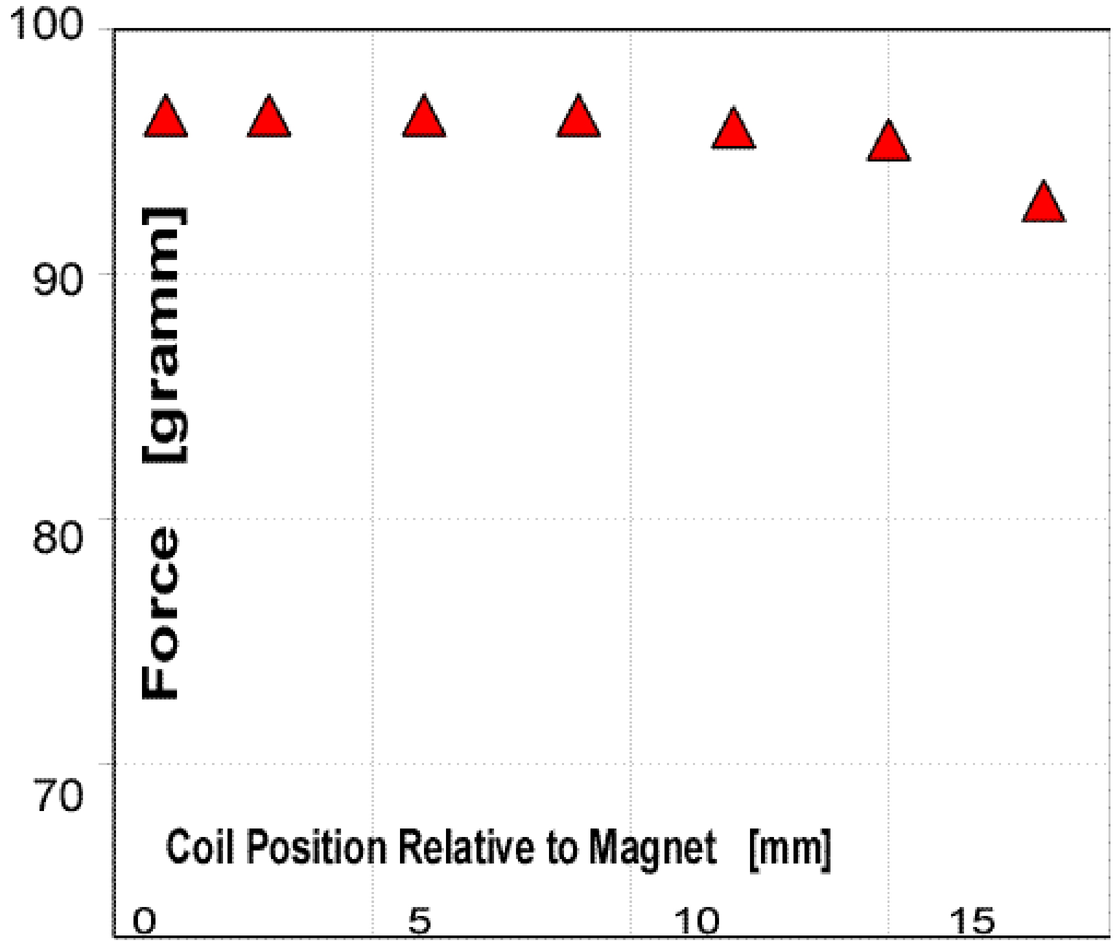

Figure 15: Force versus position measurement of the electromagnetic IP actuator. The actuator produce a force constant within less than a percent for IP movements in the horizontal plane over a rectangle 10 mm wide and 25 mm long. The force is constant also for 2 mm of vertical displacement.

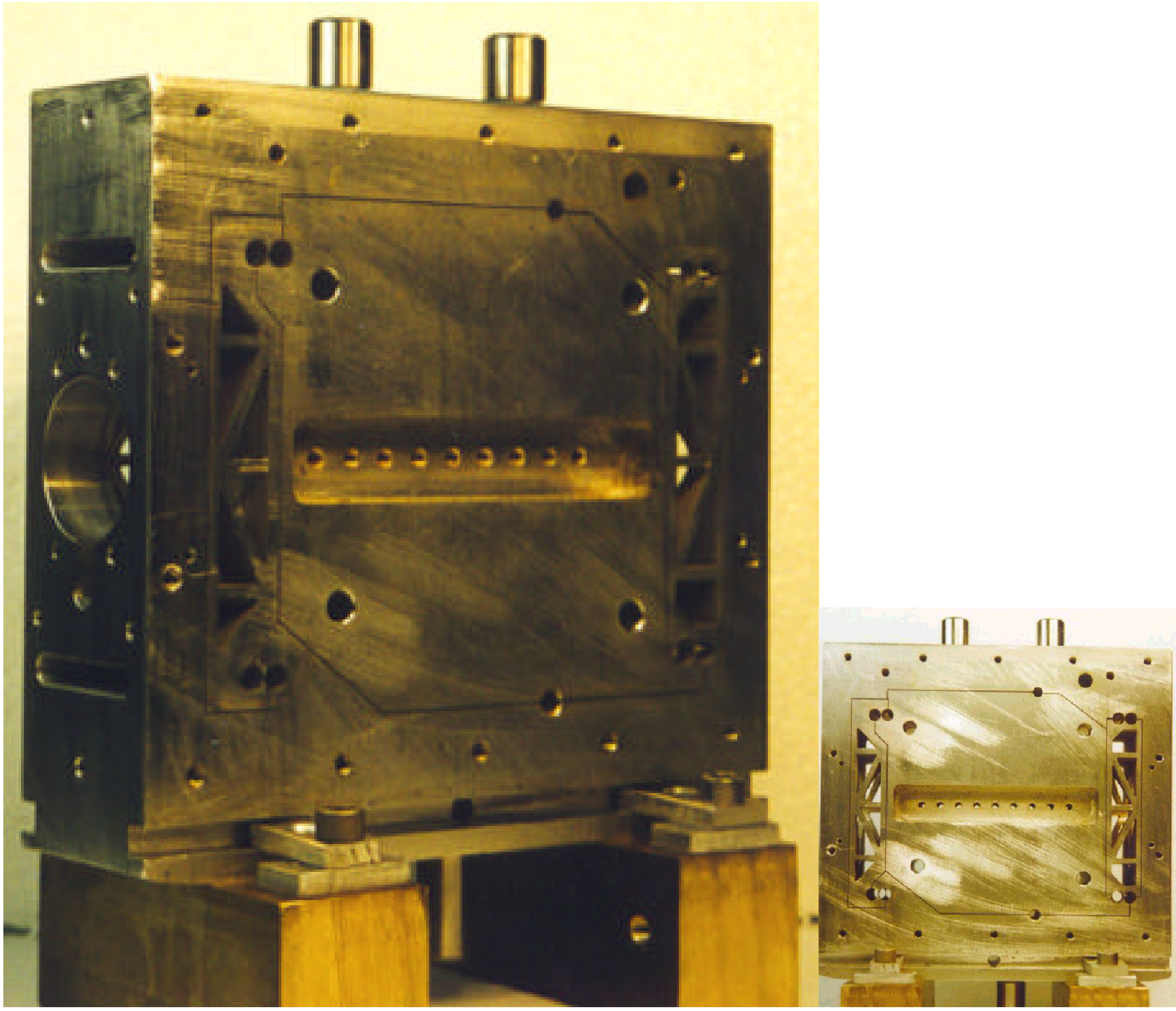

Figure 16: Photo of a monolithic horizontal accelerometer.
Visible are the test mass (center), the inverted pendulum arm (foreground arm), the pendulum arm (farther arm) and one of the two the sensor/actuator wells (left, front, in the larger image only) reaching from the outer shell to the test mass through the two arms. The 30-micron-thick eight flex joints (four visible) are the “00” shaped structures at the two extremities of the two arms. The accelerometer can be tuned to 0.2-0.5 Hz horizontal oscillation frequency. The three rods above and below the instruments are transport stops.

The problem for the IP inertial controls was solved with the monolithic, folded pendulum accelerometer shown in figure 16. The accelerometer test mass is read out with a capacitive motion sensing driving an electromagnetic feedback actuation. The accelerometer's longitudinal resonant frequency can be tuned well below 0.5 Hz and its first unwanted resonance (rotation around the transversal axis) is 23 Hz. The mechanical rejection factor of 50,000 is further increased by the sensor's insensitivity to the transversal motions. The monolithic geometry makes for extremely low mechanical thermal noise and very good UHV compatibility. The flex joints are carved with the wire EDM technique and the EDM cut residuals have been eliminated from the flex joint surface by electro-polishing, in order to improve the joints thermal noise performances.
The present sensitivity curve is shown in figure 17. It is presently limited by the sensor noise, it should be improved by a factor of at least 30 by implementing a differential capacitive sensor readout scheme currently under test. The actuator noise and flex joint thermal noise are both expected to be more than two orders of magnitude below the sensitivity curve shown. The accelerometer's sensing and actuation loop has been optimized for reliable operation as an IP feedback signal source. A further improvement in sensitivity, down to the accelerometer's flex joint thermal noise is possible by reducing its actuator strength and its dynamic range, but this may render it operational only in pre-stabilized environments.
The accelerometer development is the subject of the doctoral thesis of Alessandro Bertolini of University of Pisa.

Diagonalized position sensing of the IP

The three IP LVDT position sensors are positioned at 120^o and therefore do not point in the direction of the three IP degrees of freedom. Position signal proportional to the movement in the desired directions is obtained by a process of diagonalization performed by a DSP processor. The resulting "virtual' sensors each measure the movements of the IP in the "direction" of one of its eigen-modes and present up to 3 orders of magnitude insensitivity to the orthogonal directions as shown in figure 18. A good graphical demonstration of the diagonalization quality is shown in figure 19, where ring-down of two eigen modes is monitored independently without visible beatings.

Diagonalized actuation of the IP

In order to reduce the MIMO controls into several separated Single Input Single Output (SISO) loops it is necessary to also generate virtual actuators that push in the same "direction" of the virtual sensors measuring along the eigen-modes. Moderate diagonalization, at the level of ten percent, proved sufficient to allow effective diagonalized controls. Improvements in the diagonalization, if needed, can be obtained by an iterative process as already done in Virgo. This measurement is also limited by the air currents in the test hall.

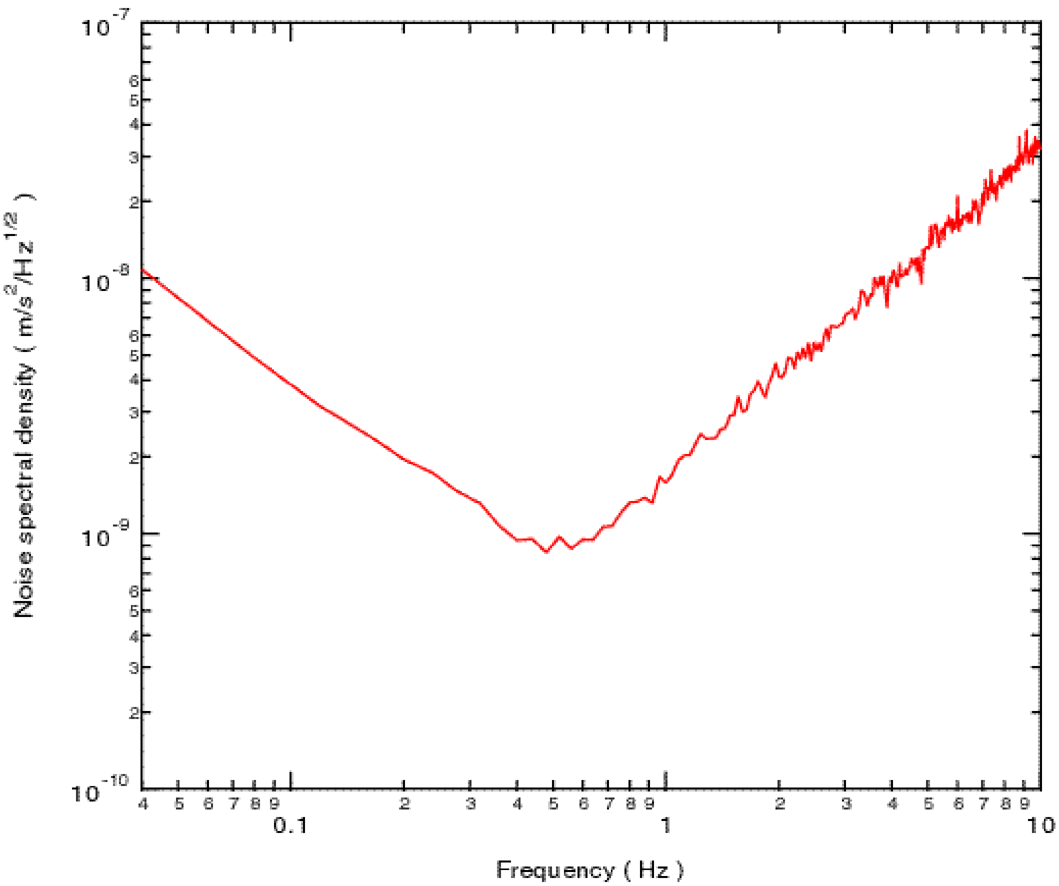

Figure 17: Present sensitivity curve of the horizontal accelerometer. The test mass resonant frequency is tuned at 0.5 Hz. The achieved resolution already exceeds the requirements of the IP inertial damping.

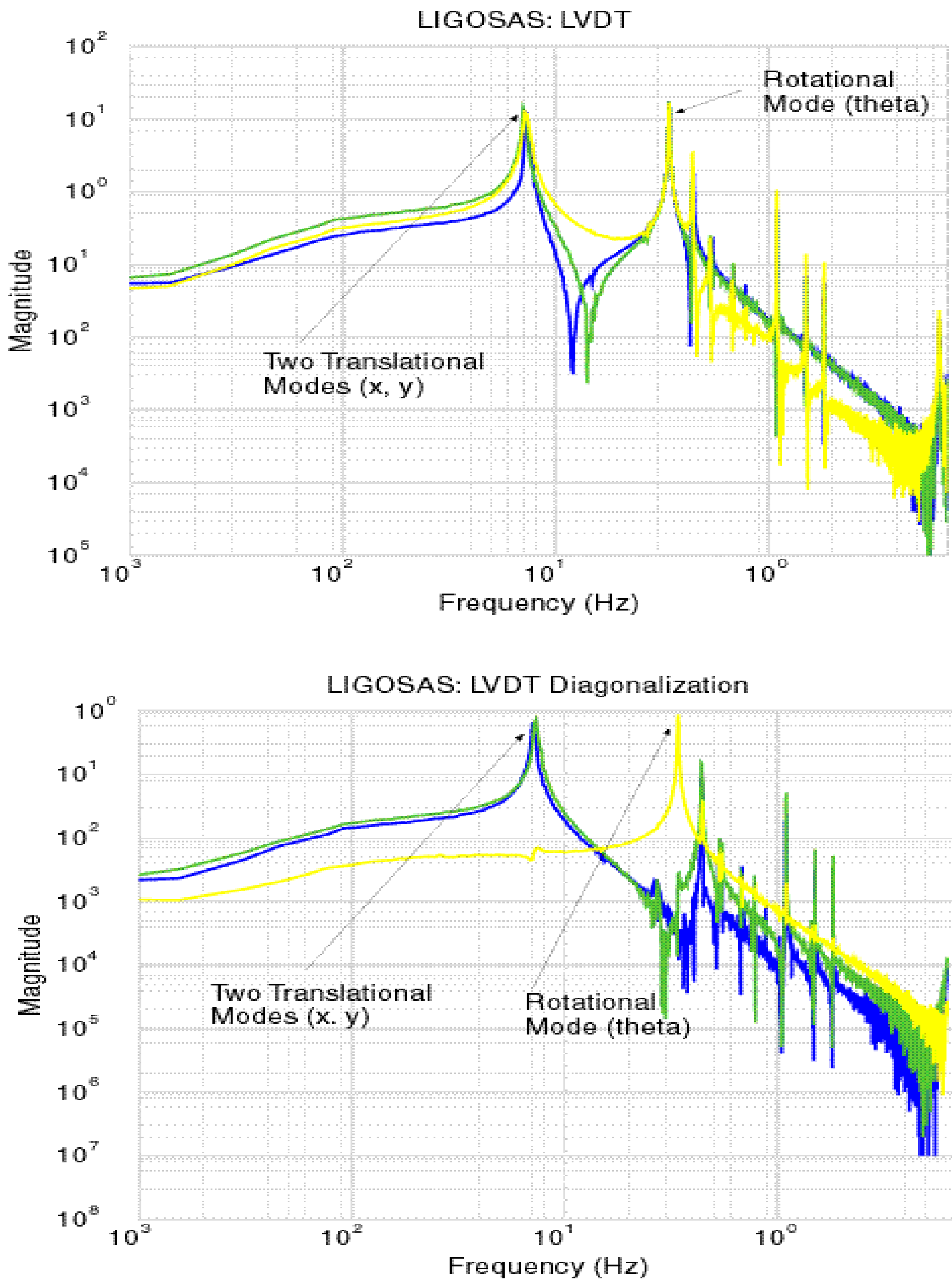

Figure 18: Frequency spectrum of the IP motion as recorded by the 3 physical LVDTs (top). The three LVDTs, placed at 120^{o}, all see the three IP eigen-modes with similar amplitudes. After the diagonalization process the three virtual LVDTs each sees only one of the IP eigen-modes and is blind to the other two.

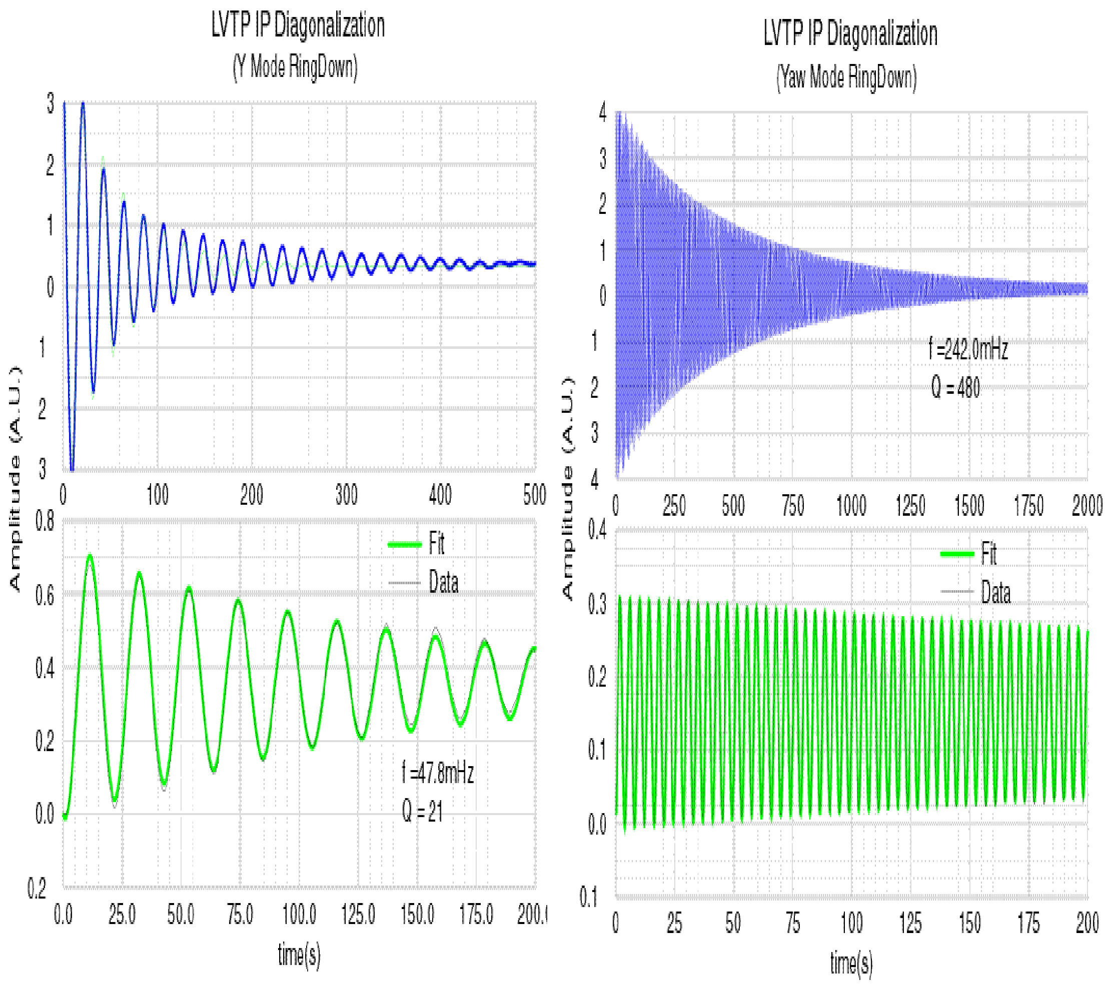

Figure 19: Ringdown of one of the two diagonalized translational modes of the IP (left) and of the rotational modes. No beating is visible between these two modes nor with the other translational one.

Diagonalized accelerometer sensing of the IP

The same is true for the accelerometers, the accelerometer signal in a previous test tower and with less performing accelerometers showed good diagonalization. This measurement is limited by the air currents in the test hall.

MIMO control of the IP

Positioning of the mirror suspension point and inertial damping or the chain's rigid modes are made in the IP MIMO feed back loop. Controls are much easier in the IP's 3 degrees of freedom than in earlier 6 d.o.f. control attempts (made in Virgo) because in the IP there is no sensors cross talk between tilt and horizontal translation (within the limits of the legs parallelism) that are particularly difficult to deal with.

Damping the modes in 3 d.o.f. does not mean missing any of the chain modes. In a chain there do not exist separate translational and tilt modes. To understand this consider for example the center link of a chain that moves purely in tilt while the ends are excited purely translationally. The 3 d.o.f. IP controls then naturally access all the chain's rigid body d.o.f., except the vertical one (note: some internal modes of the suspensions like the differential modes of the mirror-recoil mass system are, naturally, also invisible to the IP inertial damping).

In the vertical direction control is achieved through an LVDT/voice coil pair mounted coaxially in the top filter. Inertial damping is not necessary in this d.o.f. because the vertical resonances are at sufficiently low frequency that the cantilever spring present sufficiently low quality factor.

MIMO controls have not yet been implemented on a complete TAMA chain, but they have being successfully studied in the earlier and larger Advanced LIGO SAS prototype tower. Given the extensive knowledge already accumulated on the TAMA system, no significant problems are anticipated from the TAMA SAS tower controls.

Double pendulum development

The double pendulum suspension is an advancement from the present, and well tested, TAMA suspensions. It relies on an auxiliary magnetic bob to damp the movements of the intermediate mass. Both the auxiliary bob and the intermediate mass hang from a top mass attached to the SAS attenuation chain. The LIGO contribution in this design is only in the suspension mode of the intermediate mass. In order to lower the mirror pitch mode frequency (which is presently one of the worse noise limitations in TAMA), the four intermediate mass suspension wires are attached to four mini-MGAS springs, each tuned to the desired load and 1 Hz resonant frequency. These springs are two-blade springs directly derived from the three-blade springs in the MGAS filters and behave very similarly. A mini-MGAS blade being pre-tuned for insertion is shown in figure 20 and their tuning properties are shown in figure 21

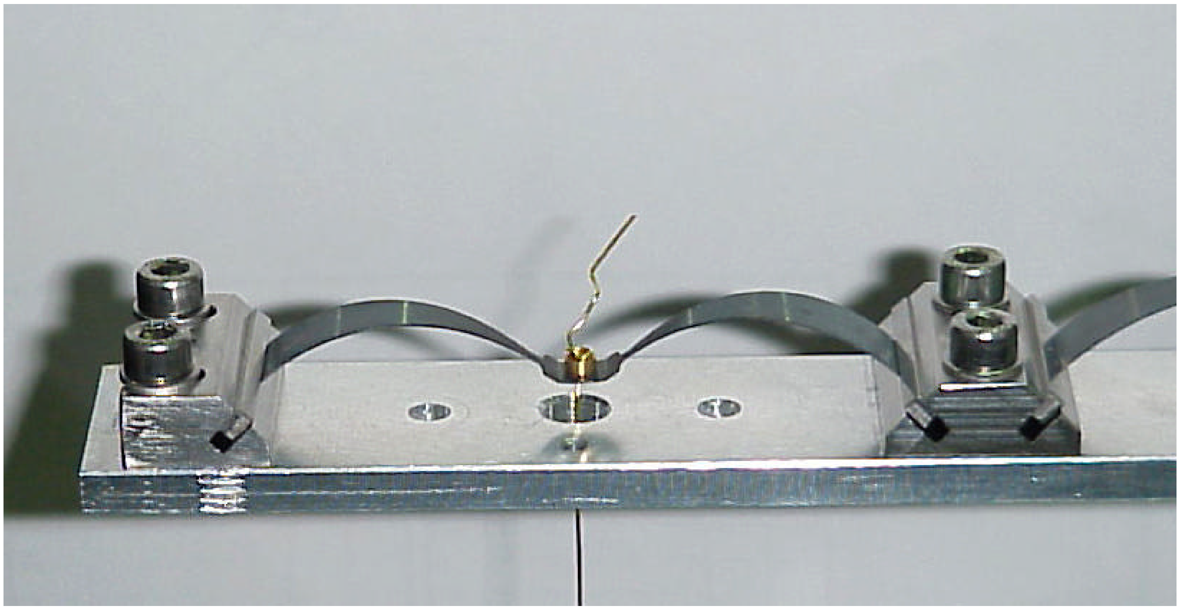

Figure 20: One of twin mini-MGAS blade being tuned for insertion in the TAMA mirror suspensions.

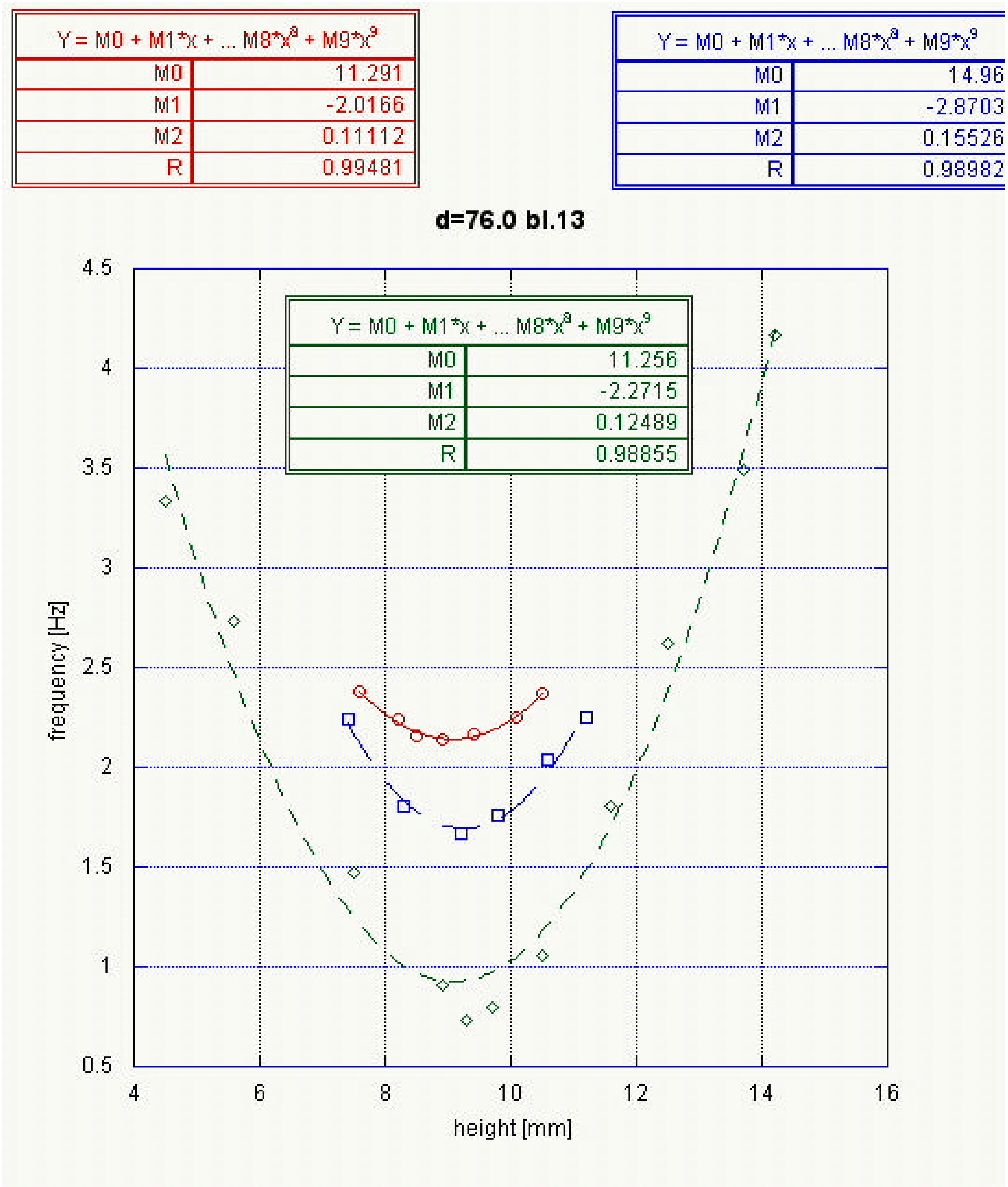

Figure 21: Tuning curve of a mini-MGAS spring in the top mass of the double pendulum mirror suspension system.

Simulation of TAMA SAS performance.

A comprehensive simulation program, based on the measured performance of the components already tested and of a simulation of the remaining parts, was performed. The expected TAMA SAS/SUS performances are illustrated in figures 22 to 25.

Figure 22 shows the expected spectral IP and mirror displacement noise. The mirror residual seismic noise crosses the floor of the thermal noise at 10Hz.

Figure 23 shows the integrated r.m.s. noise, which dictates the dynamic range requirements of the double pendulum actuators and gives the residual mirror velocity before lock acquisition. At 0.1 Hz, well below the fastest chain resonance, the projected residual motions is of few tens of nm. This small residual motion dramatically reduces the actuation dynamic range requirements and possibly opens the doors for photon drive mirror controls during the interferometer operation (electrostatic mirror actuation would be used during lock acquisition).

Figure 24 shows the expected IP control loop structure. During interferometer operation the longitudinal control loop would be slaved, from DC to up 10-100 mHz, directly to the interferometer length error signal and the control loop structure will be correspondingly modified.

Figure 25 illustrates the sensitivity improvement expected with the SAS system. The main improvement though, is expected to come from the ease of lock and increased reliability of the interferometer operation. With the current seismic attenuation system TAMA is incapable of running for sizeable periods of time during weekdays and is only marginally stable by night. SAS is expected to give a large safety margin on interferometer operational stability as well as a wider reach in the low frequency region..

Advancement Status

Two complete TAMA SAS/SUS towers have been built and they are presently in the assembly phase.

Delivery of the two systems to Japan is scheduled for February 2000.

The relative electronics is either delivered or expected to be delivered in the next few days.

Installation in the 3 meter vacuum chambers is scheduled for March 2000.

The control system installation is scheduled for the months of March and April.

The 3 meter experiment should be finalized between the months of May and July, after which the construction of the TAMA 300 towers could be started.

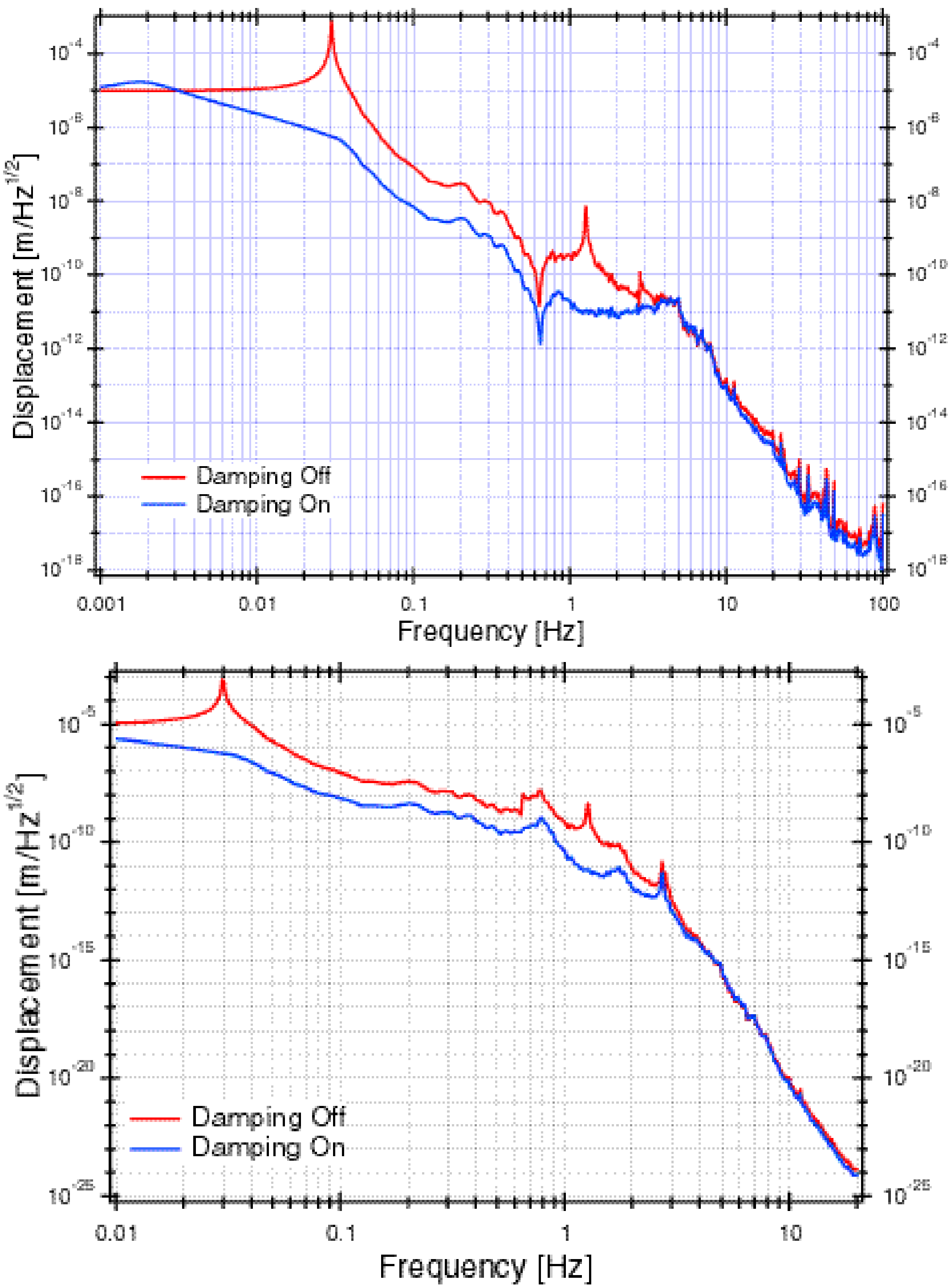

Figure 22: Simulated spectral displacement noise of the TAMA SAS IP (top) and at the mirror level (bottom).

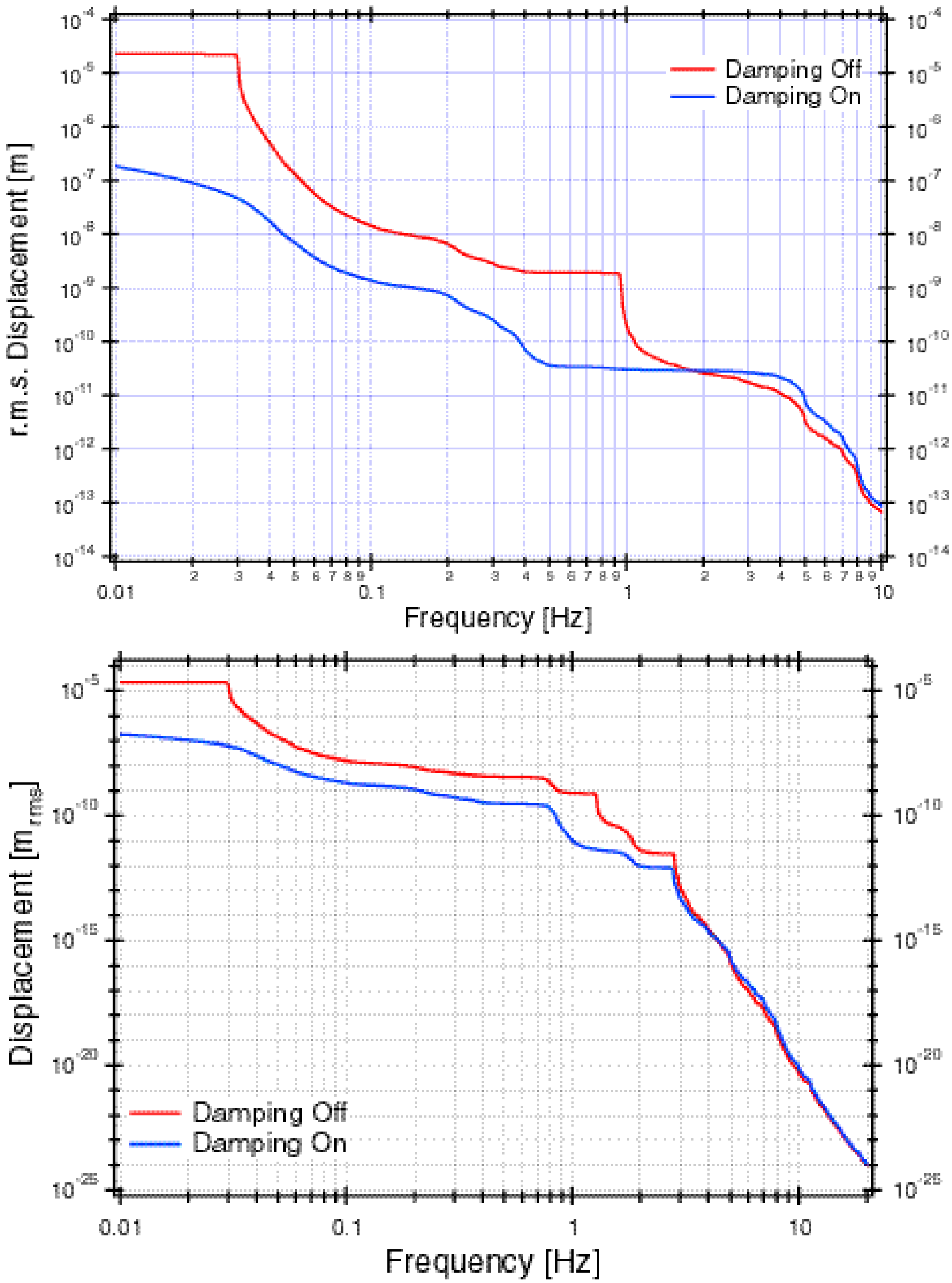

Figure 23: Simulated integrated spectral r.m.s. displacement noise of the TAMA-SAS IP (top) and at the mirror level (bottom)

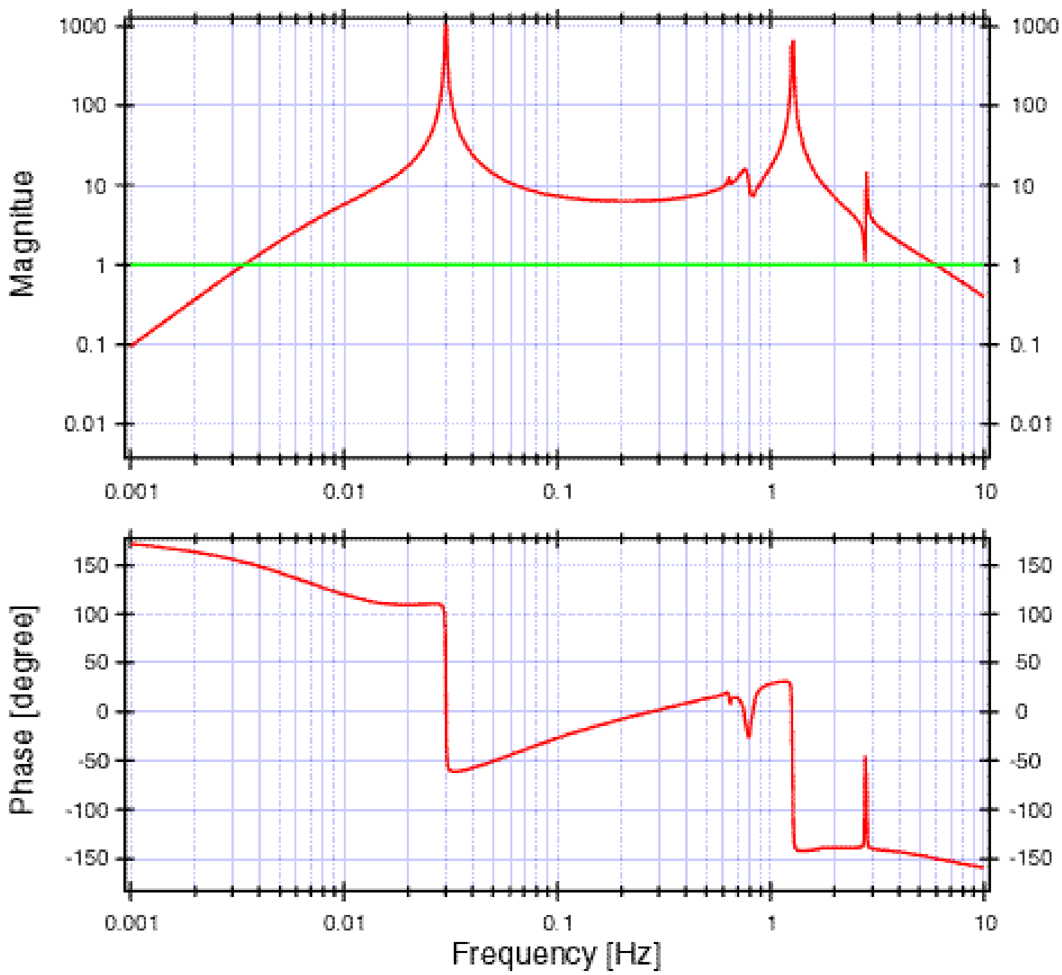

Figure 24 Control gain and phase for the inertial damping and position control loop of an IP supporting a SAS passive attenuation chain.

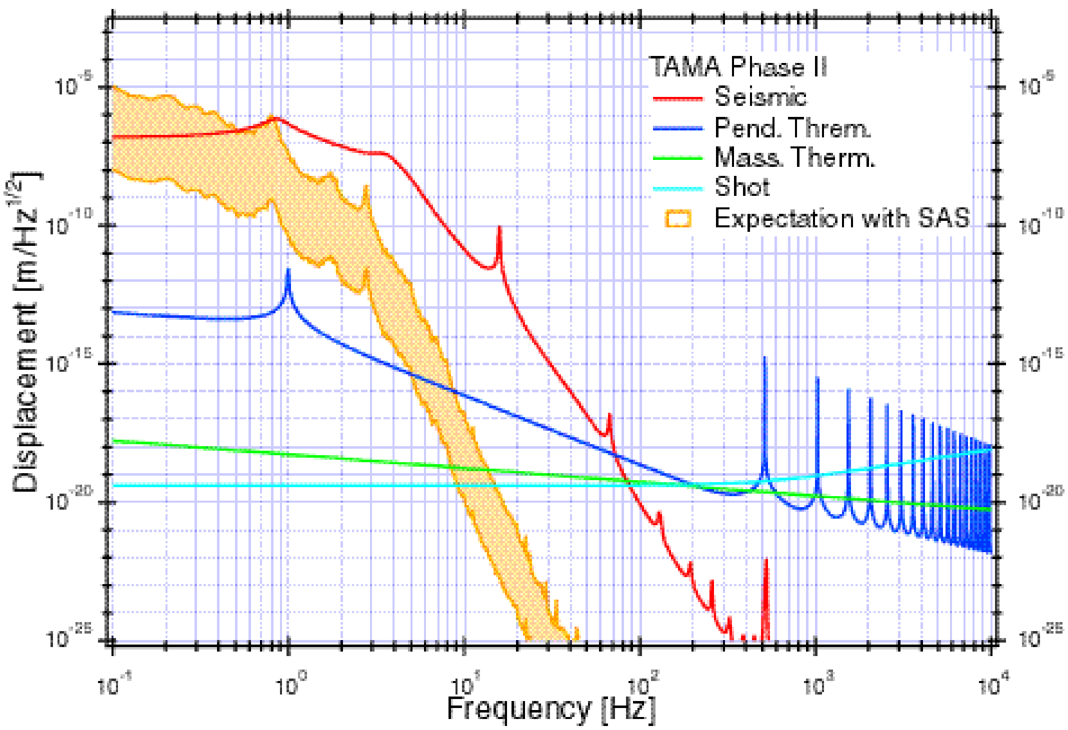

Figure 25 Simulated TAMA interferometer performance after the installation of the SAS passive attenuation chain and the new mirror suspensions (yellow band). The red curve is the present TAMA design.

Manpower, Cost and Prospects

A. Bertolini, R. DeSalvo, V. Sannibale and A. Takamori have been the principal energizers of this experiment, S. Marka, H. Tariq, N. Viboud, have already been working on this experiment for six months or more.

Eight summer students and two high school students made their internships studying different aspects of this project.

Most of the development and construction effort so far was spent in Pasadena, although a sizeable part of the accelerometer development was spent in the University of Pisa. Most of the forthcoming testing effort will be spent in the Tokyo University facility.

The first TAMA SAS prototype was obtained at LIGO expenses modifying a LIGO prototype.

The TAMA SAS/SUS towers, complete with control electronics and crates, have been built at a price of less than $ 110,000 of material costs (excluding development and manpower costs). This cost includes also the double pendulum hierarchical mirror controls and is paid by the TAMA collaboration. Some of the accelerometers are provided by the University of Pisa and LIGO.

The TAMA 3 meter and TAMA 300 tests will completely validate the SAS concept for LIGO use. A SAS/SUS system, scaled back to advanced LIGO size, excluding the fused silica suspension mechanism, would be no more complex but would cost 20 to 30% more than the TAMA system, due to the larger scale of its mechanical parts. A SAS fitting in the present LIGO vacuum envelopes would cross below the advanced LIGO thermal noise floor at 6 Hz while a slightly taller version (50% taller) would do it at 4 Hz as shown in the simulation of figure 26. Although the better performance of SAS may not be justified by the Advanced LIGO requirements, in our opinion SAS represent a good alternative solution for the seismic isolation of the Advanced LIGO test masses. SAS is ideal, if not necessary (LIGO-M000154-A, par 6.2), for the lower frequency requirements of a cryogenic LIGO, that will be difficult to satisfy with an active system.

A two in one SAS tower is presently being designed as a seismic attenuation of a pilot cryogenic thermal noise interferometer and its cold finger that could be used in a cryogenic version of LIGO, see figure 27.

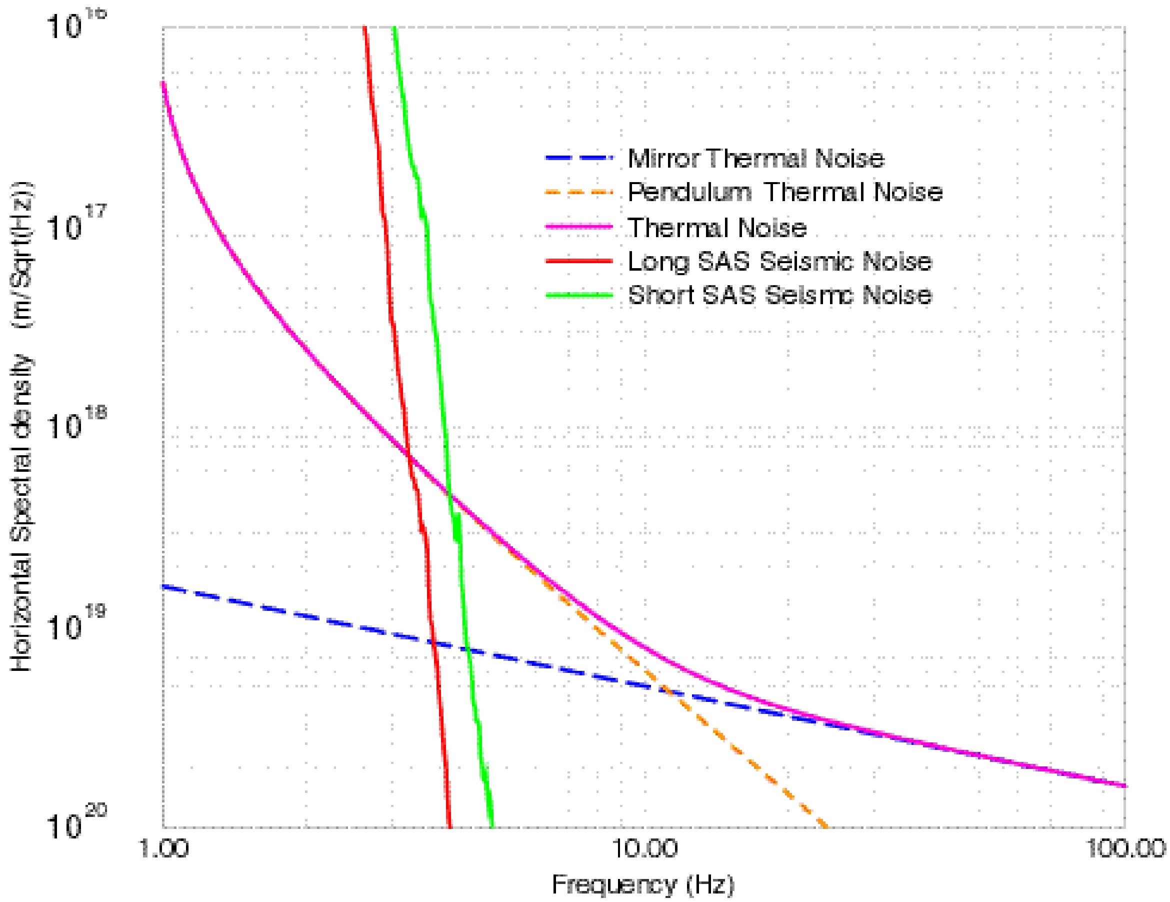

Figure 26: Simulated attenuation performance of SAS for Advanced LIGO. In green the performance of a tower fitting in the existing vacuum envelope, in red the performance of a 50% taller SAS. The thermal noise estimation is one of the Quartz Advanced LIGO estimated performances.

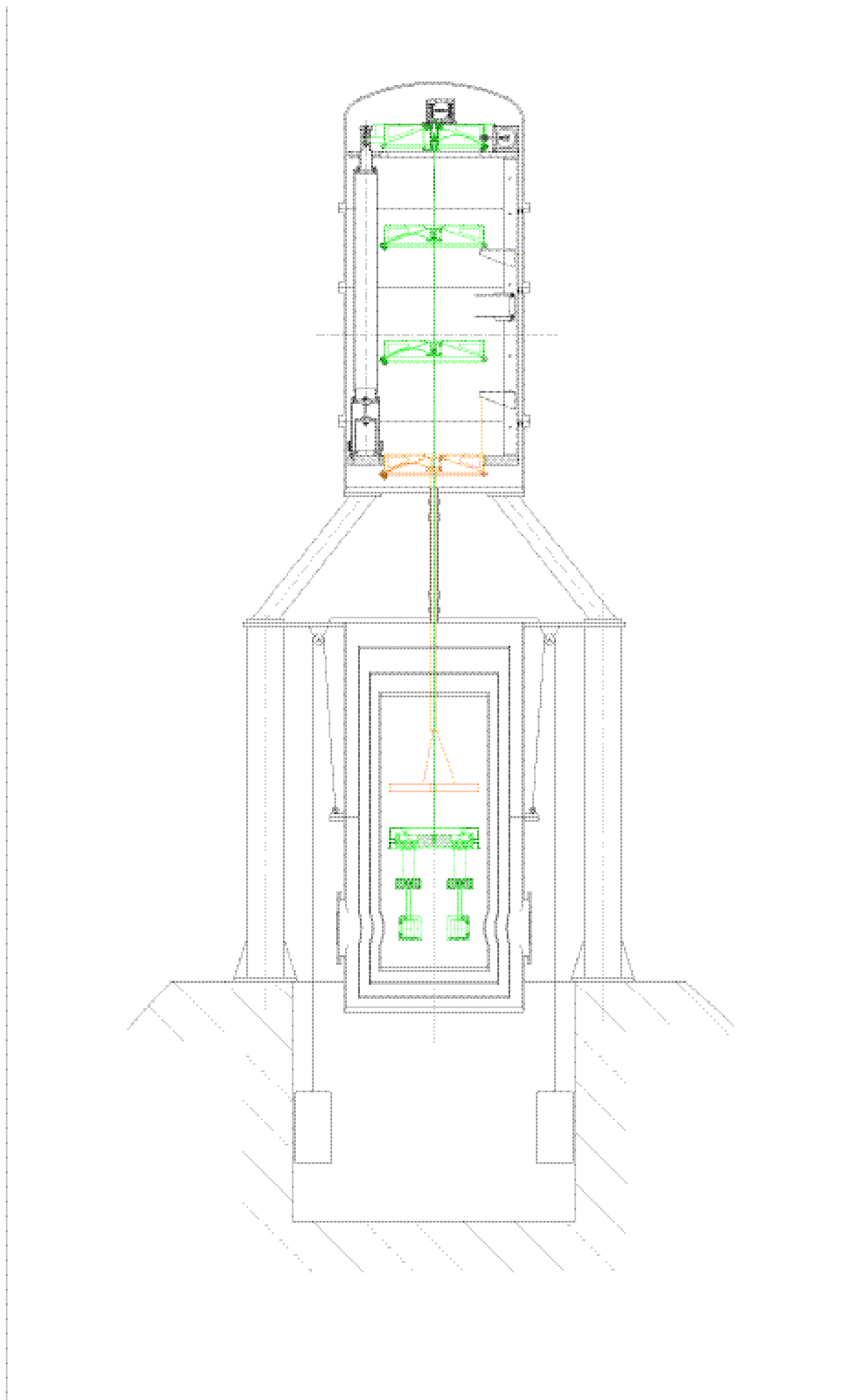

Figure 27: Tentative SAS design for a cryogenic Fabry-Perot Test at KEK. The red parts are an auxiliary seismic attenuation system for a quiet cold finger.

References to some SAS papers and reports.

**** Nuclear Instrumentation and Methods

"Seismic noise filters, vertical resonance frequency reduction with geometric anti-springs: a feasibility study", A. Bertolini, G. Cella, R. DeSalvo, V. Sannibale; Nuclear Instruments And Methods In Physics Research Section A (435)3 (1999) pp. 475-483

"Seismic isolation by mechanical filters at very low frequencies", R. DeSalvo, F. Fidecaro et.al; Nuclear Instruments And Methods In Physics Research, Section A (409)1-3 (1998) pp. 480-483

"Performances of an ultralow frequency vertical pre-isolator for the VIRGO seismic attenuation chains", R. DeSalvo, G.C. Cella, E. D'Ambrosio et.al; Nuclear Instruments And Methods In Physics, Research Section A (420)1-2 (1999) pp. 316-335 (Also available through LIGO documents)

“Progress on the R\&D Program of the Seismic Attenuation System (SAS) Proposed for the Advanced Gravitational Wave Detector, LIGO II”, V. Sannibale, et al., 8th Pisa meeting on advanced detectors, May 21-27, 2000
To be published also on Nuclear Instruments and Methods in Physics Research A 0 (2001)

****SPIE 2000

"Interferometric Gravitational Wave Detector?s Vibrational Isolation Systems", Riccardo DeSalvo et al., presented at SPIE 2000

****APS April 2000 at Long Beach, California

"Advanced Seismic Attenuation System for the LIGO II Gravitational Wave Interferometric Detector", Riccardo DeSalvo et al. ,presented at APS April 2000 at Long Beach, California

"MSE: A mechanical Simulation Engine for the LIGO End to End Model, Giancarlo Cella, presented at APS April 2000 at Long Beach, California

"Performance of Geometric Anti-Spring Filter (GASF) for Seismic Attenuation in Advanced Gravitational Wave Detectors (Akiteru Takamori et al. ,presented at APS April 2000 at Long Beach, California

"Controls of Seismic Attenuation System (SAS) for the LIGO II Gravitational Wave Detector, Virginio Sannibale et al., presented at APS April 2000 at Long Beach, California

"Characterization of LIGO II/SAS Inverted Pendulum as Low Frequency Pre-Isolation, Szabolcs Marka et al. ,presented at APS April 2000 at Long Beach, California

"Novel Design and Preliminary Testing of Linkless Geometric Anti Spring Filter, Hareem Tariq et al. ,presented at APS April 2000 at Long Beach, California

"Monolithic Accelerometer, Alessandro Bertolini, presented at APS April 2000 at Long Beach, California

"Characterization of a Low Frequency Power Spectral Density f-g in a Threshold Multi-stable Model", Erika D'Ambrosio, presented at APS April 2000 at Long Beach, California

**** Other reports

"Low Thermal Noise Accelerometers for the Active Control of a Very Low Frequency Seismic Isolator", A. Bertolini, R. DeSalvo, F. Fidecaro, M. Francesconi, LIGO T990077-00-D

"Proposal for the SAS-SUS Active Control for the LIGO Advanced Configurations (LIGO-II)", A. Bertolini, E. Black, G. Cella, E. D'Ambrosio, R. DeSalvo, K. Libbrecht, V. Sannibale, A. Takamori, P. Willems and H. Yamamoto, T990079-00-D

"Proposal of a Seismic Attenuation System (SAS) for the LIGO Advanced Configurations (LIGO-II)", Mark Barton, Alessandro Bertolini, Eric Black, Giancarlo Cella, Eugene W. Cowan, Erika D'Ambrosio, Riccardo DeSalvo, Ken Libbrecht, Virginio Sannibale, Akiteru Takamori, Nicolas Viboud, Phil Willems and Hiroaki Yamamoto, LIGO-T990075-00-D

"Seismic Noise Filters, Vertical Resonance Frequency Reduction with Geometric Anti-Springs, a Feasibility Study", A. Bertolini, G. Cella, R.DeSalvo, V.Sannibale, LIGO-P990001-A-D